



Xi'an Jiaotong-Liverpool University
西交利物浦大学

SCHOOL OF ADVANCED TECHNOLOGY

SAT301 FINAL YEAR PROJECT

*Indoor Localization Using Wi-Fi Fingerprinting and LiDAR
Fusion with Extended Kalman Filter*

Final Thesis

In Partial Fulfillment
of the Requirements for the Degree of
Bachelor of Engineering

Student Name :	Zeyi.Li
Student ID :	2144895
Supervisor :	Kyeong Soo (Joseph) Kim
Assessor :	Limin Yu

Abstract

With the expansion of innovative spaces and the growing demand for indoor robot navigation, single Wi-Fi fingerprint-based localization methods, although low-cost and easy to deploy, are susceptible to multipath fading interference and have limited localization accuracy. In contrast, Lightlaser Detection and Ranging (LiDAR) has centimeter-level ranging accuracy, but its high cost and complex deployment limit its large-scale application.

This paper proposes an indoor high-precision localization framework that integrates Wi-Fi fingerprint recognition, deep neural networks (DNNs), LiDAR-inertial measurement unit (IMU) odometers, and extended Kalman filters (EKF). First, DNN is used to perform coarse localization on standardized Wi-Fi fingerprints to obtain preliminary position estimates. Then, a Gmapping-based simultaneous localization and mapping (SLAM) method is used to fuse IMU data, generate an occupancy grid map, and output high-frequency attitude information. Finally, a unified state vector and observation model are constructed, and an EKF prediction-update fusion structure is designed to fuse information from the three sensors to suppress Wi-Fi noise and cumulative drift errors of the IMU.

Extended Kalman filtering performs state prediction and correction by linearizing the nonlinear state transition and observation equations of the system and combining system dynamics with actual observation data to achieve accurate state estimation. In this study, EKF is used to fuse the attitude information from Wi-Fi, LiDAR, and IMU, significantly improving the robustness and accuracy of the overall localization system in complex environments.

In experiments conducted on the 6th to 8th floors of the IR Building at Xi'an Jiaotong-Liverpool University, comparisons between pure Wi-Fi, pure IMU, and EKF fusion schemes revealed that Wi-Fi localization was subject to significant trajectory fluctuations due to device frequency limitations and environmental interference, resulting in limited localization accuracy. Meanwhile, IMU trajectories exhibited gradually declining localization accuracy due to cumulative errors and gradual drift. In contrast, the EKF fusion scheme demonstrated better smoothness and stability, effectively suppressing Wi-Fi and IMU errors and maintaining high accuracy and robustness. Experimental results indicate that the EKF fusion scheme maintains trajectory stability in complex environments, validating its adaptability. It also demonstrates significantly lower localization errors than single-source solutions, proving the effectiveness of multi-source information fusion in enhancing localization accuracy and system stability.

Keywords: Wi-Fi Fingerprint Localization; Simultaneous Localization and Mapping; Multi-Sensor Data Fusion; Extended Kalman Filter; Deep Neural Networks; Indoor Localization Systems

Acknowledgements

Looking back on the past four years of my undergraduate studies, I am filled with gratitude toward everyone who has supported me and every experience that has helped me grow. First and foremost, I would like to express my heartfelt thanks to my advisor, Professor Kyeong Soo Kim. Thank you for providing me with this invaluable opportunity to continuously challenge myself academically. Your academic guidance has pointed me in the right direction for my research and inspired me to explore rigorous scientific methods. Under your support, I have not only gained valuable academic knowledge but also benefited greatly in my personal growth. I feel deeply honoured to have been your FYP student and hope to repay your trust and nurturing through my efforts.

Second, I would like to sincerely thank Dr. Zhe Tang and Dr. Sihao Li for their valuable advice and guidance on my project. Dr. Tang and Dr. Li not only provided me with unique insights during the conceptualization phase of the project but also patiently assisted me in refining and improving every detail throughout its implementation. Their support and professional guidance have significantly enhanced the quality of my research and helped me maintain confidence in the face of challenges. I am fully aware that without their assistance, my project would not have progressed so smoothly.

Finally, I would like to express my deepest gratitude to my parents. Without my parents' selfless love, none of this would have been possible. They raised me without ever asking for anything in return. I am deeply grateful for their understanding and companionship. It is their support that has enabled me to persevere in pursuing and achieving my goals.

Contents

Abstract	i
Acknowledgements	ii
Contents	iii
List of Tables.....	v
List of Figures	vi
List of Abbreviations.....	vii
1 Introduction	1
1.1 Problem Statement	2
1.2 Contributions	3
1.3 Thesis Outline	3
2 Literature Review	4
2.1 Advances in indoor localization technology without calibration	4
2.2 Construction and application of long-time data sets.....	5
2.3 Combination of deep learning and multi-sensor fusion	5
2.4 Extended kalman filter in indoor localization.....	6
2.5 Multisensor fusion technology in indoor localization systems.....	7
3 Methodology	8
3.1 Data processing and integration process	8
3.2 Hardware design	8
3.3 Wi-Fi Fingerprint-based localization using Deep Neural Networks	9
3.4 Lidar-based SLAM and IMU Integration	11
3.5 Multi-Sensor fusion via Extended Kalman Filter.....	13
3.5.1 Prediction Model	15
3.5.2 Update Model.....	17
3.5.3 Performance evaluation	19
4 Experimental Results	20
4.1 Multi-floor comparison under similar indoor settings.....	20
4.2 Full corridor trajectory evaluation on the 7th floor	26
4.3 Evaluation under reversed start and end points	29
5 Discussion and Limitations	32

6 Conclusion and Future work.....	33
6.1 Conclusion.....	33
6.2 Future Work	34
References.....	35

List of Tables

3.1	Architecture of the Wi-Fi fingerprint-based DNN model	11
4.1	7th floor localization accuracy evaluation	22
4.2	6th floor localization accuracy evaluation (MAE and MSE).....	24
4.3	8th floor localization accuracy evaluation (MAE and MSE).....	26
4.4	Accuracy assessment of localization of entire path on 7th floor	29
4.5	7th floor inverse-path localization accuracy evaluation (MAE and MSE).....	32

List of Figures

1.1	Illustration of UWB and Wi-Fi hybrid localization system [1].....	1
3.1	Overall architecture and information processing flow of a multi-sensor cooperative localization system.	8
3.2	Hardware platform components of AGV.	9
3.3	Workflow of the Wi-Fi Fingerprint-Based DNN Localization Framework.	10
3.4	SLAM mapping results for three floors of the IR building.	12
3.5	EKF State Prediction and Observation Update Flowchart.	14
3.6	Structural diagram of EKF input and status vector composition.	15
4.1	First phase indoor localization experimental path	21
4.2	Comparison of experimental trajectories on the 7th floor	22
4.3	Amplified image of the error in the comparison of the experimental trajectories on the 7th floor	23
4.4	Comparison of experimental trajectories on the 6th floor	23
4.5	Amplified image of the error in the comparison of the experimental trajectories on the 6th floor	24
4.6	Comparison of experimental trajectories on the 8th floor	25
4.7	Amplified image of the error in the comparison of the experimental trajectories on the 8th floor	26
4.8	Second phase indoor localization experimental path	27
4.9	Comparison of experimental results trajectories in the entire corridor on the 7th floor of the IR building.....	28
4.10	Enlarged image of the comparison error in the entire corridor on the 7th floor of the IR building	29
4.11	Indoor localization experiment path after changing location	30
4.12	Complete path comparison of IR building 7th floor experiment trajectory (start and end locations swapped).....	31
4.13	Enlarged image of the comparison error in the entire corridor on the 7th floor of the IR building (start and end locations swapped).....	32

List of Abbreviations

AGV Autonomous Guided Vehicle

AP Access Point

CDAE Convolutional Denoising Autoencoders

CNNs convolutional neural networks

DbDIO Dual-branch Deep Inertial Odometer

DNNs Deep Neural Networks

EKF Extended Kalman Filter

GPS Global Positioning System

IMU Inertial Measurement Unit

IOT Internet of Things

LiDAR LightLaser Detection and Ranging

MAE Mean Absolute Error

MSE Mean Squared Error

ReLU Rectified Linear Unit

ROS Robot Operating System

RSSI Received Signal Strength Indication

SLAM Simultaneous Localization and Mapping

1 Introduction

Global Positioning System (GPS) is widely known for its high accuracy and broad applicability in outdoor environments. However, its limitations in indoor environments have also been well documented [2]. GPS signals are transmitted by satellites and face significant challenges in indoor spaces because they must penetrate physical obstacles such as walls and ceilings. The complexity of this transmission path causes severe signal attenuation, making it challenging to maintain a stable connection. In addition, multipath interference caused by reflections from surfaces such as walls and metal objects introduces additional time delays and computational errors, further reducing localization accuracy [2]. These challenges have prompted researchers to develop alternative indoor localization technologies aimed at overcoming these limitations and providing accurate and efficient solutions for indoor environments.

With the continuous development of modern indoor localization technologies, including Wi-Fi, Bluetooth Low Energy (BLE), Ultra Wide Band (UWB), and inertial measurement units (IMUs), significant progress has been made in many fields [3]. These technologies have significantly improved the accuracy and efficiency of indoor localization by adopting advanced methods such as triangulation, fingerprint recognition, and sensor fusion. As shown in Fig. 1.1, a typical UWB and Wi-Fi hybrid localization system contains a variety of observation data.

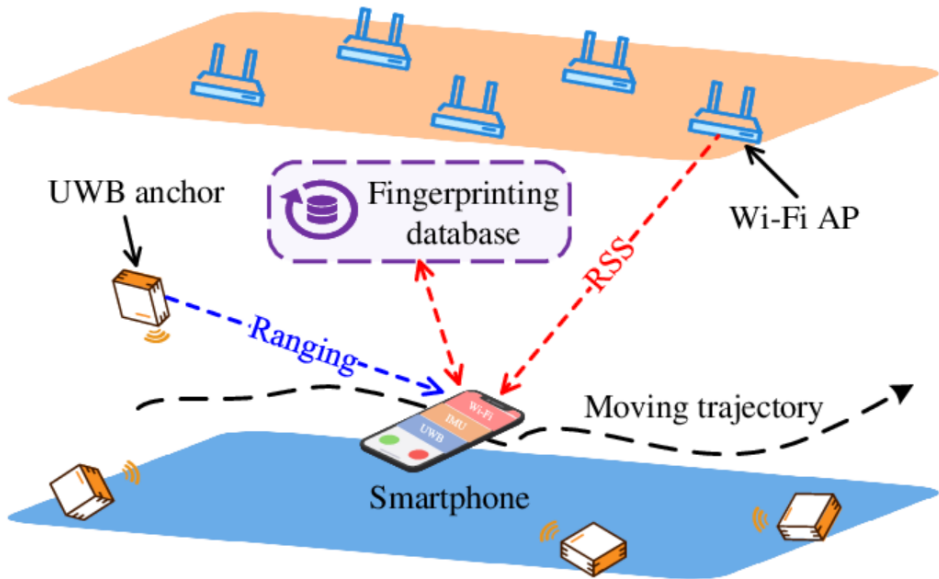


Figure 1.1: Illustration of UWB and Wi-Fi hybrid localization system [1].

In addition, indoor localization technology is widely used in the medical field for hospital material management and medical resource tracking, thereby improving the efficiency of medical services [4]. Similarly, emergency responders (such as firefighters) use these technologies to navigate in complex and unfamiliar environments, significantly improving task efficiency and safety [5]. In addition, recent advances have expanded the application of indoor localization

systems to smart cities, helping urban infrastructure management and public safety through real-time tracking and monitoring of assets and personnel [6]. These technologies have also shown significant results in the retail industry, improving the customer experience through location-based services (such as precision marketing and inventory management) [7].

Due to the limitations of GPS in indoor environments, indoor localization technology has become a key solution for achieving high-precision localization due to its flexibility, adaptability, and wide range of applications. In the following section, I introduce a new indoor localization solution and briefly describe how it is based on Wi-Fi fingerprinting, SLAM and Lidar fusion, and EKF technology.

1.1 Problem Statement

Currently, common indoor localization technologies each have their own characteristics and limitations. UWB technology measures the propagation time by sending high-frequency pulse signals and has extremely high localization accuracy [8]. However, walls and obstacles easily block UWB radio frequency signals, and signals can rapidly attenuate, especially in indoor environments where multipath effects are significant. In addition, UWB technology requires high hardware costs and dense installation infrastructure, limiting its popularity in certain applications [9].

Wi-Fi localization is a low-cost and easy-to-deploy indoor localization technology that mainly uses Wi-Fi fingerprinting or time difference of arrival (TDOA) methods to achieve localization [10, 11]. However, Wi-Fi fingerprinting requires pre-measurement of signal strength at different locations and the establishment of a fingerprint database, which is a time-consuming and complex process. In addition, Wi-Fi signals are susceptible to multipath effects and obstacles, resulting in reduced localization accuracy in complex indoor environments.

IMU localization technology estimates the displacement and attitude of an object by measuring acceleration and angular velocity. Classic IMU localization methods include physical methods (such as double integration) [12], dead reckoning methods [13], Kalman filtering [14], and sensor fusion methods [15]. However, these methods are susceptible to error accumulation (such as drift effects) during long-term use, resulting in a gradual decrease in localization accuracy. Nevertheless, IMU localization technology has high accuracy and real-time performance in a short period of time, making it particularly suitable for fast localization tasks in dynamic environments [16]. In addition, IMU technology does not rely on external infrastructure and has strong independence and reliability, making it particularly suitable for use in environments where GPS signals cannot be received, such as underground facilities, tunnels, or indoors [17]. Single indoor localization technologies have their advantages and disadvantages, but by integrating multiple sensor data, especially Wi-Fi and IMU, their limitations can be effectively compensated for, thereby achieving longer, more continuous, and more accurate localization. Currently, most research focuses on PDR/Wi-Fi fusion localization methods [18], but IMU/Wi-

Fi fusion methods based on EKF are still rare.

1.2 Contributions

The objective of this study is to develop a new indoor localization system that combines Wi-Fi, Lidar, and EKF technologies to improve localization accuracy in dynamic environments. Specifically, this study addresses the limitations of existing technologies in terms of accuracy and adaptability, providing a more powerful solution suitable for complex indoor environments.

- *DNN-based Wi-Fi localization* : This study proposes a Wi-Fi localization method based on deep neural networks (DNN) that achieves higher accuracy in indoor localization by learning the relationship between Wi-Fi signal strength (RSSI) and location.
- *Gmapping-based SLAM algorithm* : This study uses a Gmapping-based SLAM algorithm combined with Lidar data to achieve efficient real-time localization and environment mapping, improving the system's adaptability in dynamic environments.
- *Extended kalman filter data fusion* : This study uses EKF to fuse data from multiple sensors such as Wi-Fi, Lidar, and IMU, further improving the accuracy and stability of the indoor localization system. In particular, it can effectively reduce errors and signal drift in complex dynamic environments.
- *Verification of system performance through actual experiments* : This study demonstrates the application effectiveness and practical feasibility of the proposed system in complex indoor scenarios through experiments conducted in actual indoor environments.

1.3 Thesis Outline

This thesis is divided into six parts. The first part is the introduction, which provides the overall background and motivation for the project. The second part is a literature review, which comprehensively reviews the progress of indoor localization technology, data set construction, sensor fusion methods, and the application of EKF in indoor localization. The third part introduces in detail the specific methods used in this study, including Wi-Fi localization, Lidar data processing, and EKF data fusion technologies. The fourth part presents the experimental results and evaluates the localization accuracy and stability of the system in different environments. The fifth part discusses the results of the entire project, analyzes the advantages and limitations of the method, and proposes directions for improvement. Finally, the sixth part summarizes the main contributions of this research and gives prospects for future research.

2 Literature Review

In recent years, indoor localization technology has gradually become a hot topic of research in academia and industry due to its key role in applications such as smart city construction, indoor navigation, and the Internet of Things (IoT). The performance of localization systems in terms of accuracy, robustness, and system scalability directly affects their usability and deployment efficiency in real-world scenarios. With the continuous advancement of sensor technology, wireless communication, and intelligent algorithms, research in this field is showing a multidimensional trend toward integration, intelligence, and high precision.

2.1 Advances in indoor localization technology without calibration

Traditional indoor localization methods, such as Wi-Fi or Bluetooth-based fingerprinting systems, typically rely on prior site surveys to construct radio frequency (RF) maps. This process is both time-consuming and labor-intensive, and highly sensitive to environmental changes, limiting its scalability and adaptability [19]. Additionally, as environmental factors change (e.g., furniture rearrangement), the data from site surveys often becomes outdated, significantly impacting system performance [20].

To overcome these limitations, researchers have proposed calibration-free indoor localization systems. These systems avoid cumbersome site surveys by constructing RF maps using existing infrastructure or with the implicit participation of users, thereby greatly reducing deployment time and costs while improving system flexibility in dynamic environments [4, 21]. Although systems that do not require calibration offer significant advantages, they still face challenges in adapting to environmental changes and handling device heterogeneity. As emphasized by Hossain and Soh, changes in the physical environment and differences in device hardware can affect the accuracy of localization systems, posing a significant challenge for current technologies [4]. To address these issues, researchers have proposed several improvements, including dynamically updating RF maps and using advanced optimization algorithms to enhance system robustness and reliability [22].

Advances in these technologies have enabled calibration-free indoor localization technologies to be widely used in complex commercial and public environments. For example, in large shopping malls, hospitals, museums, and multi-story office buildings, the deployment and long-term maintenance of traditional localization methods are difficult due to complex building structures, high personnel mobility, and wireless signal interference. However, calibration-free systems can quickly adapt to these changing environments and provide accurate localization services by utilizing existing wireless infrastructure (such as Wi-Fi or Bluetooth) and data from mobile devices (such as smartphones) [23, 24].

2.2 Construction and application of long-time data sets

One of the core challenges facing indoor localization research is the volatility of signal strength over time. Factors such as access point configuration changes, dynamic environmental changes (e.g., crowd density, furniture movement), and device heterogeneity can significantly affect the stability and accuracy of traditional fingerprint-based localization systems [19]. Therefore, how to maintain localization accuracy in dynamic environments over long periods of time has become an urgent issue. In response to this challenge, recent research has emphasized the importance of building long-term datasets to capture the evolution of signals over time. Mendoza-Silva et al. [25] provided a Wi-Fi fingerprint dataset collected over 15 months, systematically revealing the long-term impact of factors such as network device replacement and environmental structure changes on the performance of localization systems. The study shows that incorporating long-term signal data into a fingerprint database and updating it dynamically can significantly improve the system's ability to adapt to environmental changes, thereby reducing localization errors caused by signal attenuation or configuration drift. To achieve real-time adaptation, many scholars have proposed mechanisms for dynamically updating fingerprint databases. For example, Zhang et al. [26] and Bahl et al. [27] proposed using time modeling and online learning algorithms to dynamically maintain RF maps, enabling the system to respond in real time to changes in the signal environment and avoid the accuracy degradation issues commonly found in static fingerprint systems. The combination of long-term data sets and adaptive updating mechanisms has greatly improved the robustness and reliability of localization systems. In particular, in highly dynamic real-world scenarios such as multi-story buildings, shopping malls, or large transportation hubs, this strategy can ensure that the system continues to provide high-precision localization services [28, 29], effectively responding to the challenges brought about by environmental uncertainty and changes.

2.3 Combination of deep learning and multi-sensor fusion

In recent years, deep learning technology has made breakthroughs in fields such as computer vision and natural language processing. Inspired by this, researchers have begun to introduce it into indoor localization systems, especially in scene recognition and precise localization tasks in complex environments. Unlike traditional methods that rely on static fingerprint matching, deep learning can automatically extract multi-level features from multi-sensor data through neural networks, model more complex spatial patterns, and thus improve the system's adaptability and robustness [30, 31].

Liu et al. proposed an indoor localization method that integrates deep convolutional neural networks (CNNs) and multi-sensor data [30]. This method is based on Wi-Fi, magnetic field, and inertial sensor data for indoor scene recognition, and estimates the user's location through a particle filtering algorithm. Experimental results show that this method can control the lo-

calization error within 1.32 meters at a 95% confidence level, which is significantly better than traditional fingerprint matching technology in dynamic environments. At the same time, this method effectively alleviates the signal ambiguity caused by environmental changes and improves the generalization ability of the system.

Traditional fingerprint localization methods rely on a pre-collected signal strength fingerprint database and estimate the location by matching it with real-time observation signals [32]. Although these methods perform well in relatively stable environments, they face several limitations: on the one hand, static fingerprint databases cannot dynamically adapt to environmental changes, such as wireless device replacement or changes in personnel density; on the other hand, these methods are highly sensitive to signal interference and multipath effects, often resulting in significant errors in multi-story buildings or densely populated areas [33].

In contrast, deep learning methods can learn robust spatial features from heterogeneous sensor data with the help of neural networks and adapt to environmental changes through incremental learning or online updates, thereby effectively maintaining localization accuracy. For example, Nowicki and Wietrzykowski proposed a CNN-based Wi-Fi fingerprint localization method that outperformed traditional methods in multiple scenarios [31]. In addition, Zhou et al. introduced long short-term memory (LSTM) networks to perform time modelling of multi-sensor signals, achieving real-time adaptive localization in complex dynamic environments [34].

2.4 Extended kalman filter in indoor localization

Extended Kalman filters are widely used in indoor localization systems as real-time recursive estimators that can fuse noisy, asynchronous, and multimodal sensor data within a probabilistic framework. Unlike the standard Kalman filter, which is only applicable to linear systems, the EKF linearizes nonlinear motion and observation models through a first-order Taylor expansion, enabling it to handle nonlinear motion and observation models. This makes it particularly suitable for indoor environments, where user trajectories, sensor measurements, and signal propagation are inherently nonlinear [35].

In Wi-Fi-based localization scenarios, EKF is often used to refine location estimates based on noisy RSSI or channel state information observations. When fused with other modalities such as IMU and Lidar, EKF can integrate absolute and relative localization information, thereby improving localization accuracy and temporal continuity [23]. For instance, the WIO-EKF method proposed by Zhou and Wang (2023) combines Wi-Fi fingerprint and IMU data [36]. It fuses them using EKF to provide more accurate and continuous pedestrian localization. The innovation of this method lies in that it not only solves the initial heading error problem of IMU, but also enhances the localization results using Wi-Fi fingerprint data. Specifically, the WIO-EKF method first enhances Wi-Fi fingerprint data using the CDAELoc model (a regression network based on convolutional denoising autoencoders) to improve the robustness of Wi-Fi localization in noisy environments. Then, the DbDIO model (a dual-branch deep inertial

odometer network) is used to process IMU data and accurately extract features of different scales. The prediction results of these models are input as system observations into the EKF, thereby reducing the initial heading error of the IMU system.

2.5 Multisensor fusion technology in indoor localization systems

With the continuous evolution of indoor localization technology, traditional localization methods that rely on a single signal source face significant challenges in terms of accuracy and robustness in complex environments. In order to improve the stability and adaptability of the system in dynamic and interference-prone environments, multi-sensor fusion technology has gradually become an important direction for indoor localization system research and application. This technology integrates data sources from different types of sensors to achieve more accurate, continuous, and robust estimation of the target location.

Multi-sensor fusion can be categorized into three typical architectures: data-level fusion, feature-level fusion, and decision-level fusion. Data-level fusion directly integrates raw sensor data, retaining the most complete information, but requires high time synchronization and noise robustness. Feature-level fusion combines features extracted independently by each sensor, balancing complexity and efficiency. Decision-level fusion performs final estimation through weighted voting or filtering strategies after each subsystem completes localization inference, and is suitable for heterogeneous or distributed systems [37].

Currently, multi-sensor fusion is mainly reflected in several key application paths: First, Wi-Fi and IMU fusion compensates for the drift of Wi-Fi localization in short-term dynamic changes through inertial measurement units (such as accelerometers and gyroscopes) and is widely used in areas without GPS signal coverage [38]. Second, UWB and vision (camera or LiDAR) fusion is suitable for industrial scenarios or robot path planning and can achieve centimeter-level localization accuracy [39]; third, deep learning-assisted fusion frameworks learn the nonlinear relationships between multimodal features in end-to-end models through neural networks to achieve robust perception and localization in complex environments [34].

Although fusion technology has significantly improved the performance of localization systems, many challenges remain [37]. First, the issues of time synchronization, coordinate alignment, and scale consistency between different sensors have not been completely resolved. Second, given the limited computing power of mobile devices, the computational complexity and energy efficiency optimisation of fusion algorithms still need to be balanced. Finally, multi-sensor systems face practical deployment challenges such as data heterogeneity and outlier handling, which affect their feasibility in large-scale, low-cost application scenarios.

3 Methodology

3.1 Data processing and integration process

In order to achieve a high-precision and robust indoor localization system, this paper designs and implements a localization method framework that integrates information from multiple sensors. The overall process covers the entire process from raw data collection and information fusion processing to localization result optimization. The system uses multiple sensors such as Wi-Fi, Lidar, and IMU for collaborative localization, and realizes multi-source data fusion and optimization estimation through the EKF algorithm.

The entire data acquisition and fusion process is divided into several steps: First, data from different sensors (such as Wi-Fi signals, SLAM maps, and IMU data) are collected, preprocessed, and stored in a database. Then, these data are fused and optimized through the EKF algorithm to ultimately achieve accurate localization estimation. Fig. 3.1 shows the detailed steps of data acquisition, sensor data fusion, and localization result optimization..

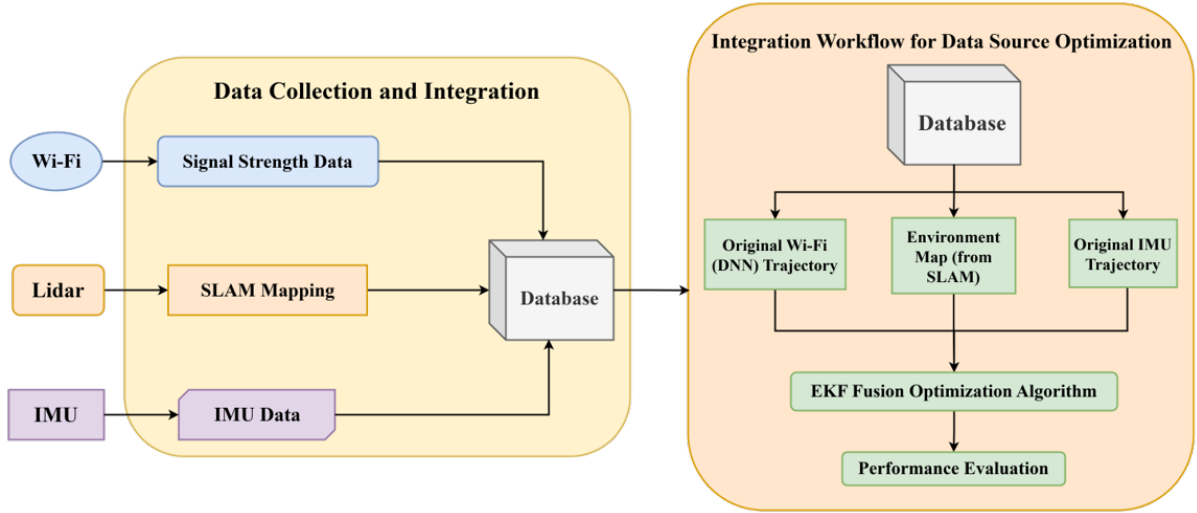


Figure 3.1: Overall architecture and information processing flow of a multi-sensor cooperative localization system.

In the next section, I introduce the deployment and integration of this localization system on an autonomous mobile platform, including the hardware and software architecture design, module docking process, and system operation mechanism, thereby verifying the applicability and feasibility of this method in a real environment.

3.2 Hardware design

The localization system in this study is deployed on a mobile autonomous platform, namely an autonomous guided vehicle (AGV), which serves as a carrier for multi-sensor data acquisition

and real-time localization. As shown in the Fig. 3.2, the AGV platform consists of three main components: a mobile chassis system, a sensor module, and an edge computing unit. Among them, the mobile chassis is equipped with differential drive motors and wheel encoders, which provide good steering flexibility and motion stability, enabling smooth movement and path tracking in indoor environments. The sensor module integrates a two-dimensional laser radar, IMU, Wi-Fi receiver, and depth camera to perceive the environmental structure, capture its dynamic state, and obtain wireless signal information. The computing core of the system consists of edge computing units (such as NVIDIA Jetson and Raspberry Pi), which are responsible for local data collection and processing.

The entire platform is compact in design and easy to deploy flexibly in multi-story and multi-scenario environments, providing a good hardware foundation for subsequent large-scale localization experiments and system expansion. After data collection is complete, one of the core issues of this research is how to efficiently integrate data from different sensors to ensure localization accuracy and robustness.

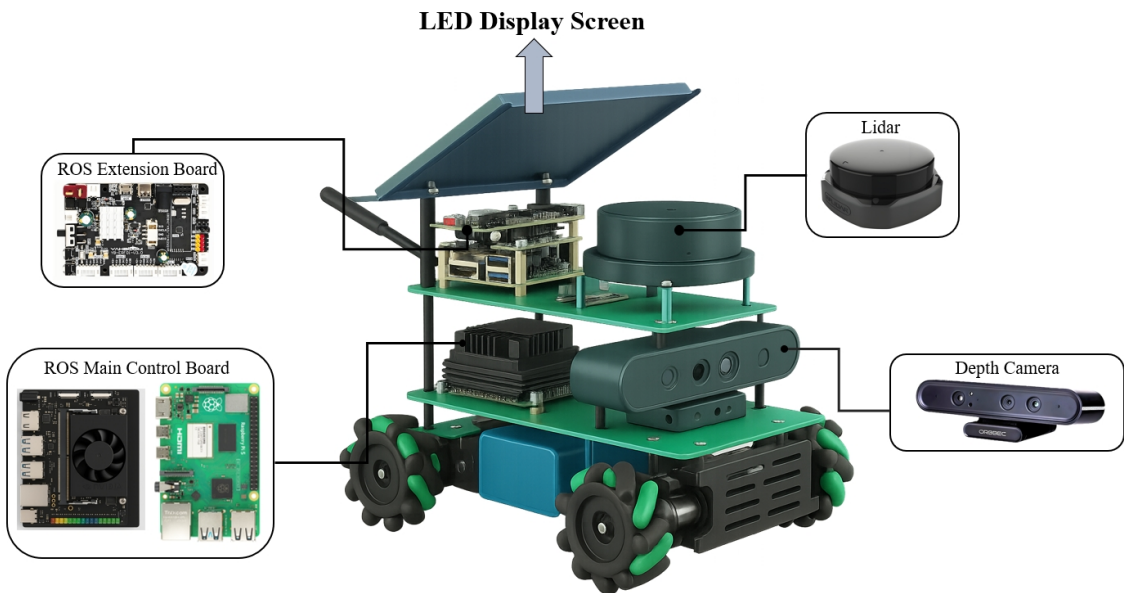


Figure 3.2: Hardware platform components of AGV.

3.3 Wi-Fi Fingerprint-based localization using Deep Neural Networks

On the basis of multi-source data collection and system integration, this study further constructed a Deep Neural Networks (DNNs) model based on Wi-Fi Received Signal Strength Indication (RSSI) fingerprints to achieve regression prediction of the platform's two-dimensional location. The model aims to characterize the nonlinear mapping relationship between RSSI signal strength and physical space coordinates, and to model high-dimensional RSSI feature vectors through a supervised learning framework, thereby achieving high-precision indoor localization.

As shown in the Fig. 3.3, the overall process of the Wi-Fi localization subsystem is divided into four stages: data preparation, feature modelling, model training and prediction, and performance evaluation, which constitute a complete fingerprint-based localization method.

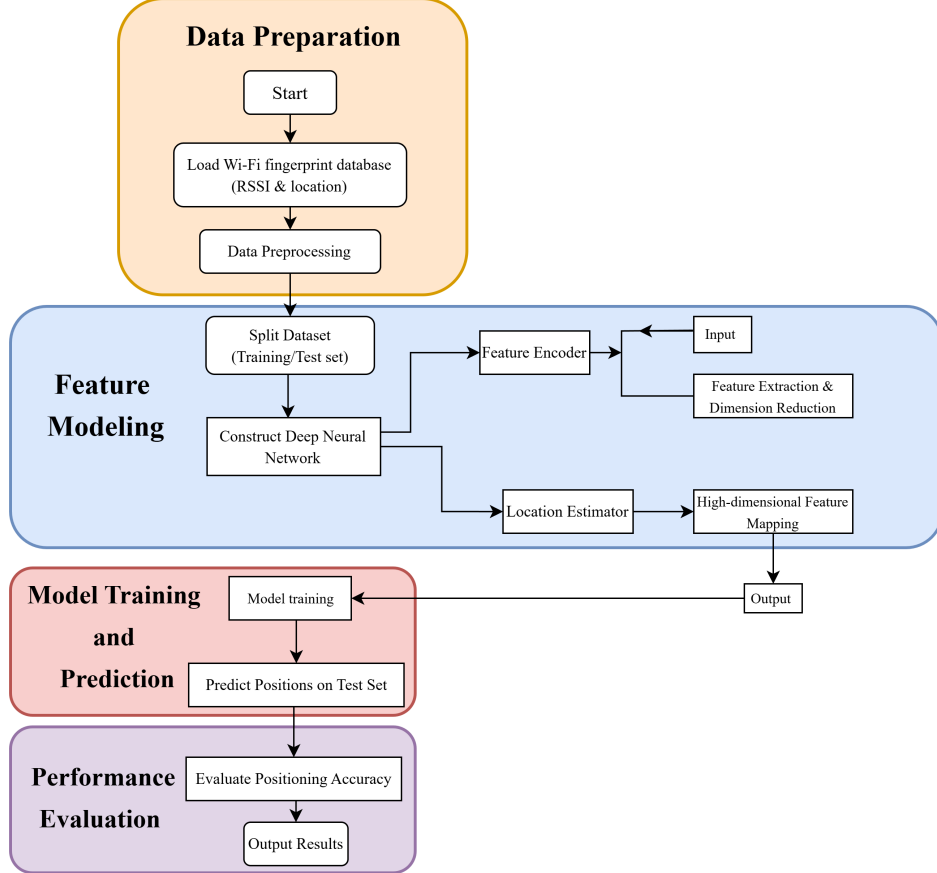


Figure 3.3: Workflow of the Wi-Fi Fingerprint-Based DNN Localization Framework.

First, the system loads a pre-built fingerprint database, which contains RSSI vectors collected at different reference points and their corresponding physical coordinate labels. To improve modelling quality and convergence stability, the raw data is preprocessed, including missing value filling, feature normalization, and outlier removal. After preprocessing, the data is divided into training and testing sets for subsequent model learning and generalization capability verification.

In the modelling phase, this study designed a multi-layer feedforward neural network structure to extract spatial features from high-dimensional RSSI fingerprints and perform location regression prediction. The model consists of multiple linear layers, Rectified Linear Unit (ReLU), and dropout layers, constructed using a layered stacking method of “Linear-ReLU-Dropout.” The input dimension of the network is 219, corresponding to the number of active access points (AP), and the output is a two-dimensional coordinate value (x, y). The complete network layer structure is shown in the Table. 3.1. This structure can effectively extract potential spatial distribution patterns in the signal space and achieve mapping from the signal domain to the

physical domain.

Table 3.1: Architecture of the Wi-Fi fingerprint-based DNN model

Layer	Type	Input Dim	Output Dim	Activation / Dropout
1	Linear	219	109	ReLU + Dropout(0.2)
2	Linear	109	73	ReLU + Dropout(0.2)
3	Linear	73	54	ReLU + Dropout(0.2)
4	Linear	54	109	ReLU + Dropout(0.2)
5	Linear	109	109	ReLU + Dropout(0.2)
6	Linear	109	109	ReLU + Dropout(0.2)
7	Linear	109	2	None

During the model training process, the mean squared error (MSE) is used as the loss function, and the Adam optimizer is used to update the model parameters. In the testing phase, the model receives RSSI vector input and outputs the location prediction results. Then, the average localization error is calculated by comparing the Euclidean distance between the predicted location and the actual coordinates to evaluate the model's performance.

Overall, as an essential part of the localization system, the Wi-Fi fingerprint localization framework not only provides prior trajectory information for the subsequent fusion stage but also demonstrates good robustness and generalization ability, making it suitable for a variety of complex and dynamically changing indoor environments.

3.4 Lidar-based SLAM and IMU Integration

Although Wi-Fi fingerprint-based deep neural network models can achieve relatively accurate location estimates in static environments, they still face many challenges in complex indoor environments, including severe RSSI fluctuations, multipath propagation, signal obstruction, and high fingerprint database update costs. These factors can easily lead to a decline in model generalization performance, especially in areas with sparse or dynamically changing signals, where it is difficult for the system to maintain continuous and stable localization output.

To enhance the system's environmental perception and spatial understanding capabilities, this study introduces the SLAM method. SLAM can construct an environmental map and perform self-localization in real time by processing sensor observation data in the absence of prior maps, and is widely used in mobile robots and indoor navigation systems [40]. Its core idea is to dynamically update the environment representation while estimating the platform trajectory, thereby achieving joint inference of space and motion.

In this system, we specifically adopted the particle filter-based Gmapping algorithm. Gmapping uses Rao-Blackwellized particle filtering technology to fuse two-dimensional laser radar scan data with wheel odometer information, and utilizes a probabilistic grid mapping method to

generate a closed-loop consistent, high-resolution two-dimensional environmental map, and outputs high-precision pose trajectory estimates [41]. Compared with other methods, Gmapping has the advantages of mature implementation, low computational resource consumption, and strong closed-loop detection capabilities, making it particularly suitable for real-time mapping tasks in small and medium-sized indoor scenes.

Fig. 3.4 shows the environment map results obtained by the system when performing SLAM mapping on the 6th, 7th, and 8th floors of the IR building at Xi'an Jiaotong-Liverpool University (XJTLU). The results clearly reproduce the floor structure and reflect the coverage area of the laser scan.

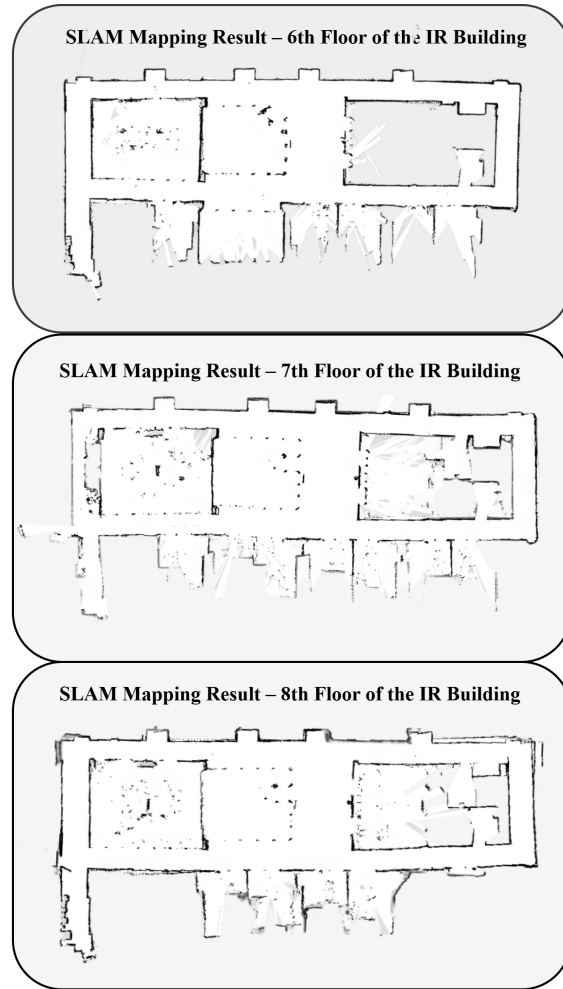


Figure 3.4: SLAM mapping results for three floors of the IR building.

For further improvement of the system's dynamic response capabilities under conditions of rapid movement, turning, and partial obstruction, an IMU is integrated into the localization system as an auxiliary sensor. IMU usually includes a three-axis accelerometer and a three-axis gyroscope, which are used to measure linear acceleration and angular velocity. Through integration, the attitude changes and displacement information of the platform in a short period

of time can be estimated.

$$\boldsymbol{a} = \begin{bmatrix} a_x \\ a_y \\ a_z \end{bmatrix}, \quad \boldsymbol{\omega} = \begin{bmatrix} \omega_x \\ \omega_y \\ \omega_z \end{bmatrix} \quad (3.1)$$

where a_x, a_y, a_z denote the accelerations along the x-, y-, and z-axes, respectively. $\omega_x, \omega_y, \omega_z$ denote the angular velocities about the x-, y-, and z-axes, respectively.

In the modelling process, IMU observation data is represented as:

$$\boldsymbol{a}_{\text{meas}} = \boldsymbol{a}_{\text{true}} + \boldsymbol{b}_a + \boldsymbol{n}_a, \quad \boldsymbol{\omega}_{\text{meas}} = \boldsymbol{\omega}_{\text{true}} + \boldsymbol{b}_\omega + \boldsymbol{n}_\omega \quad (3.2)$$

where, $\boldsymbol{a}_{\text{meas}}$ denotes the observed acceleration, $\boldsymbol{a}_{\text{true}}$ denotes the true acceleration, \boldsymbol{b}_a denotes the zero bias, and \boldsymbol{n}_a denotes the noise term. Similarly, $\boldsymbol{\omega}_{\text{meas}}$ represents the measured angular velocity, $\boldsymbol{\omega}_{\text{true}}$ is the true angular velocity, \boldsymbol{b}_ω is the corresponding bias, and \boldsymbol{n}_ω accounts for measurement noise. These sources of error are modelled and corrected during the fusion stage using the EKF to improve localization stability and accuracy. The high sampling frequency of the IMU enables it to effectively compensate for the shortcomings of Lidar in short-term motion estimation, improving the localization continuity and robustness of the system in highly dynamic environments.

Overall, the integration of SLAM and IMU not only provides a solid foundation for the system to construct an environmental map and provide continuous trajectory estimation, but also provides structured and dynamic compensation multi-source perception support for subsequent fusion optimization with Wi-Fi trajectories.

3.5 Multi-Sensor fusion via Extended Kalman Filter

This study further constructs a fusion framework based on the EKF to achieve effective coordination and information complementarity among subsystems. The fusion model is centered on state space modeling, integrating pose information from Wi-Fi fingerprint localization, SLAM module outputs, and short-term high-frequency motion observations provided by IMU sensors to achieve dynamic estimation and real-time correction of the platform state.

In the specific implementation, the EKF models the nonlinear motion system as a recursive prediction-update structure, alternately completing the two stages of state estimation and observation correction. The prediction stage infers the future state of the system based on the state at the previous moment and the control input, while the update stage corrects the state based on sensor observations, thereby continuously improving the estimation accuracy. This filtering structure has been widely applied in multi-sensor fusion localization and demonstrates good robustness in addressing issues such as IMU drift and RSSI instability [42].

The recursive process of the overall state estimation is shown in the Fig. 3.5 below.

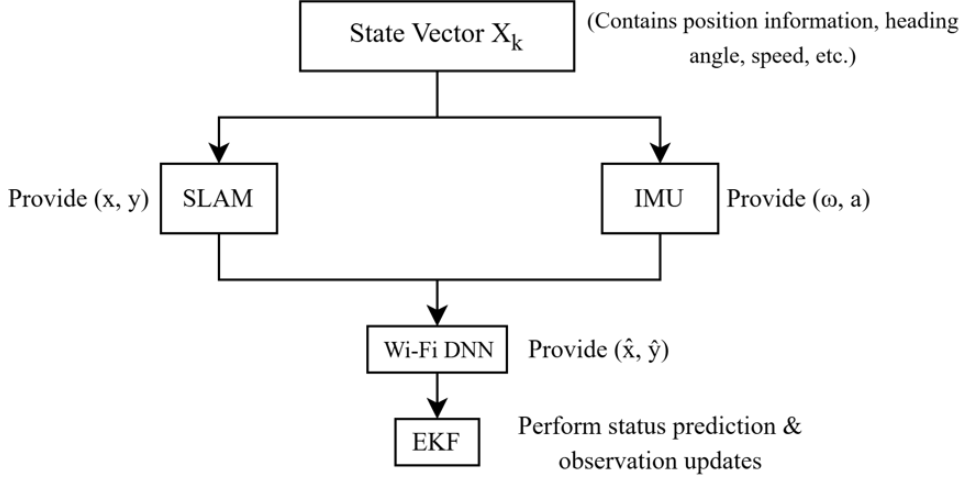


Figure 3.5: EKF State Prediction and Observation Update Flowchart.

All formulas in this section are based on the EKF model structure and state estimation framework proposed in the literature [43, 44, 45] and are used to model the multi-sensor data fusion process. To establish a unified estimation system, it is first necessary to define the system state vector and its evolution relationship. In this study, the system state estimated by the EKF is defined as

$$\mathbf{X}_k = \begin{bmatrix} x_k \\ y_k \\ \theta_k \\ v_k \\ \omega_k \end{bmatrix} \quad (3.3)$$

where the platform's position (x_k, y_k) in the two-dimensional plane, heading angle θ_k , linear velocity v_k , and angular velocity ω_k , constituting a complete description of the motion characteristics.

Different from traditional methods, which typically estimate only two-dimensional locations as state variables [46], this study further introduces dynamic motion parameters (velocity and angular velocity), enhancing the system's ability to model continuous trajectories, especially in highly dynamic or complex path environments, with stronger robustness [47].

Specifically, the two-dimensional location estimation (x_k, y_k) of the platform is mainly obtained by the Wi-Fi fingerprint localization module through RSSI vector modelling. Although its update frequency is low, it has good global stability and long-term consistency. The SLAM module outputs the estimated results of the mid-frequency trajectory containing the position and orientation angle θ_k through the joint mapping of the laser radar and odometer, providing structured spatial constraints for the system. The linear velocity v_k and angular velocity ω_k of the platform are mainly derived from the high-frequency dynamic measurements of the accelerometer and gyroscope in the IMU module, which can be used for short-term motion inference and

compensation in the state prediction phase. The relationship between each subsystem and the state vector is shown in the Fig. 3.6 below.

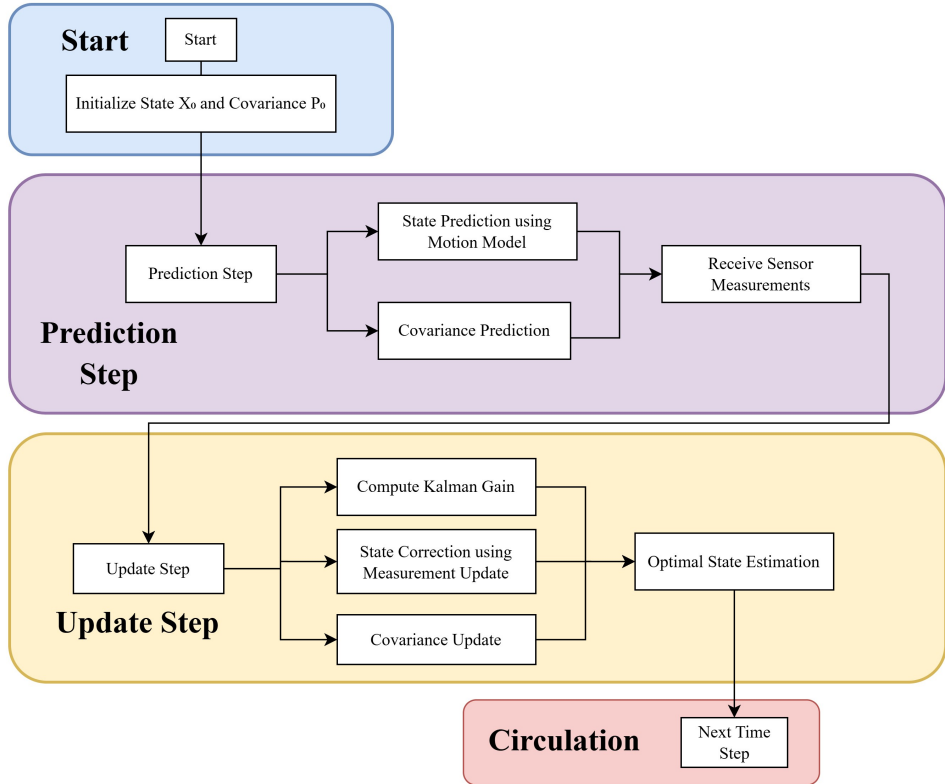


Figure 3.6: Structural diagram of EKF input and status vector composition.

Based on the source and characteristics of the perceived information, the system state is modelled as a nonlinear dynamic process and estimated recursively using an EKF. The following sections will detail the EKF state modelling method, including the construction of the system prediction model and observation model, as well as the role of multi-source observations in the fusion process.

3.5.1 Prediction Model

In EKF, the prediction step is used to infer the prior distribution of the current state based on the state estimate and control input at the previous moment, and to perform covariance propagation. Let the state vector be Equation 3.3, and the control input \mathbf{u}_k comes from the IMU sensor, which contains linear acceleration and angular velocity measurements.

$$\mathbf{u}_k = \begin{bmatrix} a_k \\ \omega_k \end{bmatrix} \quad (3.4)$$

where \mathbf{u}_k denotes the control input vector at time step k , consisting of the measured acceleration and angular velocity from the IMU:

- a_k : the 3D linear acceleration vector, $a_k = [a_x, a_y, a_z]^T$
- ω_k : the 3D angular velocity vector, $\omega_k = [\omega_x, \omega_y, \omega_z]^T$

According to the nonlinear kinematic model of the system, the predicted form of the state at time step k is:

$$\hat{\mathbf{x}}_{k|k-1} = \begin{bmatrix} x_{k-1} + v_{k-1} \cdot \Delta t \cdot \cos(\theta_{k-1}) \\ y_{k-1} + v_{k-1} \cdot \Delta t \cdot \sin(\theta_{k-1}) \\ \theta_{k-1} + \omega_{k-1} \cdot \Delta t \\ v_{k-1} + a_k \cdot \Delta t \\ \omega_k \end{bmatrix} \quad (3.5)$$

where $\hat{\mathbf{x}}_{k|k-1}$ denotes the predicted state vector at time step k given information up to time $k-1$. The state transition function incorporates both kinematic and dynamic updates using control inputs. Specifically:

- x_{k-1}, y_{k-1} : position coordinates at time $k-1$
- v_{k-1} : linear velocity at time $k-1$
- θ_{k-1} : heading (yaw) angle at time $k-1$
- ω_{k-1} : angular velocity (yaw rate) at time $k-1$
- a_k : linear acceleration at time k (from IMU)
- ω_k : angular velocity at time k (from IMU)
- Δt : discrete time interval

The first two rows correspond to position prediction using a constant velocity motion model; the third row updates the heading angle with angular velocity; the fourth row propagates linear velocity via acceleration; the final row directly passes the angular velocity.

$$\mathbf{F}_k = \begin{bmatrix} 1 & 0 & -v_k \Delta t \sin(\theta_k) & \Delta t \cos(\theta_k) & 0 \\ 0 & 1 & v_k \Delta t \cos(\theta_k) & \Delta t \sin(\theta_k) & 0 \\ 0 & 0 & 1 & 0 & \Delta t \\ 0 & 0 & 0 & 1 & 0 \\ 0 & 0 & 0 & 0 & 0 \end{bmatrix} \quad (3.6)$$

where \mathbf{F}_k is the first-order partial derivative of the nonlinear state transition function $f(\mathbf{x}_k, \mathbf{u}_k)$ with respect to the state \mathbf{x} (Jacobian matrix), expressed as follows:

- v_k : the current linear velocity of the robot (obtained from the control input or state variables)

- θ_k : the robot's current heading angle
- Δt : discrete time interval

Note that the first two columns of \mathbf{F}_k are constant because the position components x and y are not directly influenced by themselves in the transition function, but rather updated through the control variables v_k and θ_k . Therefore, $\partial x_{k+1}/\partial x_k = 1$ and $\partial y_{k+1}/\partial y_k = 1$, resulting in identity entries in the upper-left block of the Jacobian.

This matrix is the state transition Jacobian of the linearized state transition function $f(\mathbf{x}_k)$, used to predict state covariance. The covariance propagation formula is:

$$\mathbf{P}_{k|k-1} = \mathbf{F}_k \mathbf{P}_{k-1} \mathbf{F}_k^\top + \mathbf{Q}_k \quad (3.7)$$

where \mathbf{P}_{k-1} is the state covariance from the previous step, and \mathbf{Q}_k is the process noise covariance matrix. This prediction stage provides a dynamic prior estimate of the current state of the system, which serves as the basis for subsequent observation updates.

3.5.2 Update Model

After completing state prediction, the EKF enters the observation update phase, which introduces actual observation information from external sensors (such as SLAM or Wi-Fi) into the system state estimation. The core objective of this process is to correct the predicted state based on the current observations, thereby reducing the cumulative deviation caused by system modelling errors or process noise. Let the observation result of the sensor at time step k be z_k , and the corresponding observation model be:

$$\mathbf{z}_k = h(\mathbf{X}_k) + \mathbf{v}_k = \begin{bmatrix} x_k \\ y_k \end{bmatrix} + \mathbf{v}_k \quad (3.8)$$

where $\mathbf{z}_k \in \mathbb{R}^2$ representing a two-dimensional real-valued vector, consists of position observations from either the Wi-Fi fingerprint module or the SLAM system. $h(\mathbf{X}_k)$ is a nonlinear observation function, \mathbf{v}_k is zero-mean Gaussian noise with covariance R_k . In this study, we assume that the observations are the positions of the platform on a two-dimensional map, so the observation function is:

$$h(\mathbf{X}_k) = \begin{bmatrix} x_k \\ y_k \end{bmatrix} \quad (3.9)$$

where $h(\mathbf{X}_k)$ denotes the observation model that maps the full state vector \mathbf{X}_k to the measurable output. In this case:

- \mathbf{X}_k : the full state vector at time k , typically including position, orientation, velocity, etc.
- x_k, y_k : the 2D position coordinates extracted from the state for observation.

The Jacobian matrix of the observation model \mathbf{H}_k is a constant matrix

$$\mathbf{H}_k = \frac{\partial h}{\partial \mathbf{X}_k} \quad (3.10)$$

where \mathbf{H}_k is the Jacobian matrix of the observation function $h(\mathbf{X}_k)$ with respect to the state vector \mathbf{X}_k , evaluated at time step k . It describes the sensitivity of the observable outputs to small changes in the system state. In the case where $h(\mathbf{X}_k) = [x_k, y_k]^T$ and $\mathbf{X}_k = [x_k, y_k, \theta_k, v_k, \omega_k]^T$, the matrix \mathbf{H}_k takes the following form:

$$\mathbf{H}_k = \begin{bmatrix} 1 & 0 & 0 & 0 & 0 \\ 0 & 1 & 0 & 0 & 0 \end{bmatrix}$$

After obtaining the predicted state $\hat{\mathbf{X}}_{k|k-1}$ and the predicted covariance $\mathbf{P}_{k|k-1}$, the system first calculates the Kalman gain.

$$\mathbf{K}_k = \mathbf{P}_{k|k-1} \mathbf{H}_k^\top (\mathbf{H}_k \mathbf{P}_{k|k-1} \mathbf{H}_k^\top + \mathbf{R}_k)^{-1} \quad (3.11)$$

where \mathbf{K}_k is the Kalman gain matrix at time step k , determining how much the predicted state should be corrected based on the new observation. Specifically:

- $\mathbf{P}_{k|k-1}$: the predicted error covariance matrix before the update step
- \mathbf{H}_k : the observation model Jacobian matrix at time k
- \mathbf{R}_k : the observation noise covariance matrix

The gain matrix is used to balance prediction uncertainty and observation noise, determining the magnitude of the final state correction. Subsequently, the state vector is updated based on the observation residual

$$\hat{\mathbf{x}}_k = \hat{\mathbf{x}}_{k|k-1} + \mathbf{K}_k (\mathbf{z}_k - h(\hat{\mathbf{x}}_{k|k-1})) \quad (3.12)$$

where $\hat{\mathbf{x}}_k$ is the updated state estimate at time k after incorporating the measurement. The correction term $\mathbf{K}_k (\mathbf{z}_k - h(\hat{\mathbf{x}}_{k|k-1}))$ adjusts the prediction based on the innovation (residual) between the actual observation and the predicted observation. Specifically:

- $\hat{\mathbf{x}}_{k|k-1}$: the predicted state before the measurement update
- \mathbf{K}_k : the Kalman gain at time k
- \mathbf{z}_k : the actual observation (measurement vector)
- $h(\hat{\mathbf{x}}_{k|k-1})$: the predicted observation derived from the predicted state

This update rule ensures that the new estimate $\hat{\mathbf{x}}_k$ is a weighted combination of the prior prediction and the new measurement, accounting for their respective uncertainties.

Finally, the system synchronizes and corrects the state covariance matrix to reflect the updated uncertainty distribution.

$$\mathbf{P}_k = (\mathbf{I} - \mathbf{K}_k \mathbf{H}_k) \mathbf{P}_{k|k-1} \quad (3.13)$$

where \mathbf{P}_k is the updated error covariance matrix at time step k . It reflects the uncertainty associated with the updated state estimate. Specifically:

- \mathbf{I} : the identity matrix of appropriate dimensions

Through the above update steps, EKF can dynamically correct the platform status at each observation time, thereby achieving effective fusion of multi-source information and continuous improvement in state estimation accuracy.

Ultimately, the system can output continuous, smooth, and accurate position and attitude estimation results in real time in complex dynamic environments, achieving an organic integration of the global consistency provided by Wi-Fi and the local high-frequency dynamic perception of IMU, significantly enhancing the robustness and stability of the localization system under sensor uncertainty and environmental disturbances.

3.5.3 Performance evaluation

After completing the EKF fusion, we obtained the trajectory map after Wi-Fi, IMU, and SLAM data fusion using EKF. To further enhance the reliability of the experimental results and quantify the accuracy of the localization system after the fusion of different sensor data, this study introduced the mean squared error (MSE) and mean absolute error (MAE) as performance evaluation indicators. These two indicators reflect the accuracy and robustness of the localization system from different perspectives, thereby providing strong quantitative support for the effectiveness of multi-source data fusion.

MSE and MAE are widely used error evaluation standards in current indoor localization research, especially suitable for fingerprint localization and multi-sensor fusion scenarios, and have been widely verified by multiple studies for their effectiveness and universality [47, 48].

$$\text{MSE} = \frac{1}{N} \sum_{i=1}^N (x_{\text{true},i} - x_{\text{pred},i})^2 + (y_{\text{true},i} - y_{\text{pred},i})^2 \quad (3.14)$$

where, N is the number of test data points, $x_{\text{true},i}$ and $y_{\text{true},i}$ are the actual location coordinates of the i_{th} test point, and $x_{\text{pred},i}$ and $y_{\text{pred},i}$ are the coordinates predicted by Wi-Fi, IMU, or EKF. The mean absolute error is used to measure the absolute magnitude of the difference between the predicted value and the actual value. Compared with MSE, MAE is less sensitive to outliers and can more clearly reflect the overall accuracy of the model.

$$\text{MAE} = \frac{1}{N} \sum_{i=1}^N |x_{\text{true},i} - x_{\text{pred},i}| + |y_{\text{true},i} - y_{\text{pred},i}| \quad (3.15)$$

where $|\cdot|$ denotes absolute value, and the meanings of other symbols are consistent with those in Equation 3.14.

After calculating the error of the entire trajectory, in order to further analyse the localization accuracy of the system at certain moments, we also used a local magnification to show the specific situation at the point of maximum error. By magnifying the displayed area, we can clearly see the error between Wi-Fi and IMU and EKF, and further compare the performance of different sensors at specific locations, especially in areas where Wi-Fi localization errors are large. In order to quantitatively evaluate these errors, we used the following error calculation formula:

$$\text{Wi-Fi Error} = \sqrt{(x_{\text{EKF}}(t) - x_{\text{WiFi}}(t))^2 + (y_{\text{EKF}}(t) - y_{\text{WiFi}}(t))^2} \quad (3.16)$$

$$\text{IMU Error} = \sqrt{(x_{\text{EKF}}(t) - x_{\text{IMU}}(t))^2 + (y_{\text{EKF}}(t) - y_{\text{IMU}}(t))^2} \quad (3.17)$$

where $x_{\text{EKF}}(t), y_{\text{EKF}}(t)$ denote the 2D location estimated by EKF, and $x_{\text{WiFi}}(t), y_{\text{WiFi}}(t)$ and $x_{\text{IMU}}(t), y_{\text{IMU}}(t)$ denote the predicted location from Wi-Fi and IMU.

By using Euclidean distance for intuitive visualization, we can better understand changes in system accuracy and verify the advantages of EKF in complex environments.

4 Experimental Results

All experiments in this study were conducted on a mobile AGV platform equipped with NVIDIA Jetson computing modules, 2D lidar, an inertial measurement unit (IMU), and a Wi-Fi receiver, as shown in Fig. 3.2

4.1 Multi-floor comparison under similar indoor settings

To validate the proposed EKF-based multi-source fusion localization framework, this study conducted a series of indoor localization experiments on the 6th, 7th, and 8th floors of the IR building at Xi'an Jiaotong-Liverpool University. The experiments were mainly conducted in the corridor areas of the floors, taking into account factors such as signal obstruction and dynamic movement in the environment to test the localization accuracy and stability of the system in complex environments.

During the experiments, the platform followed a predefined trajectory while simultaneously collecting Wi-Fi RSSI, IMU, and Lidar data. Wi-Fi data was processed through a DNN model for regression, utilizing the RSSI vectors of each reference point for training to predict the corresponding location. This study set up three localization schemes for comparison:

- Using only the Wi-Fi fingerprint regression model
- Using only IMU inertial measurements

- Using EKF for localization results after Wi-Fi, IMU, and SLAM data fusion

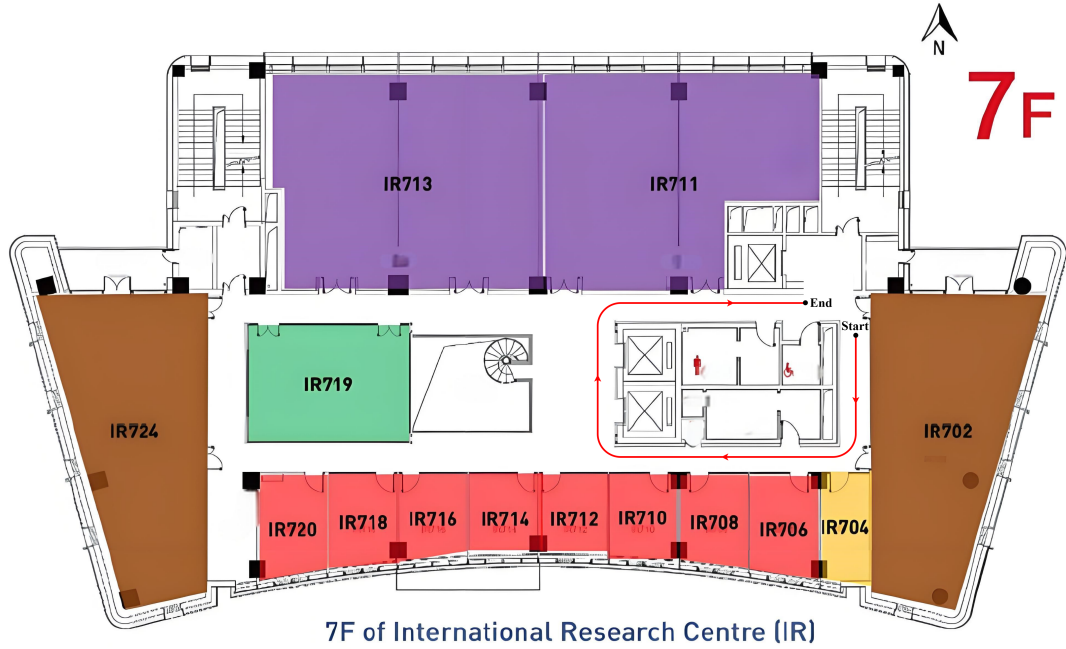


Figure 4.1: First phase indoor localization experimental path

The first phase of the experiment was conducted in similar corridor areas on the 6th, 7th, and 8th floors of the IR building. To ensure a comprehensive evaluation of the performance of different sensors, we conducted experiments in the same areas across the three floors (as shown in the Fig. 4.1), obtaining three sets of path maps that demonstrate the experimental results for the three floors. Each set of graphs shows the trajectories of Wi-Fi localization, IMU localization, and EKF fusion localization, which are distinguished by different colours and line types. The blue trajectory represents the results after EKF fusion, the orange dotted line represents Wi-Fi localization, and the green dotted line represents IMU localization results.

As shown in the Fig. 4.6, the trajectories obtained using the Wi-Fi, IMU, and EKF fusion method are displayed. In the Wi-Fi localization results, due to the influence of signal obstruction and reflection in the environment, the localization trajectory showed apparent deviations, indicating that Wi-Fi localization is susceptible to multipath propagation and signal attenuation in indoor environments. The IMU localization results showed significant errors, especially when the platform was moving quickly or turning, as the IMU system errors tended to accumulate, leading to a decrease in localization accuracy. In contrast, the EKF fusion method effectively combines the data advantages of Wi-Fi and IMU, providing smoother and more accurate trajectories through multiple corrections of state estimates and sensor data.

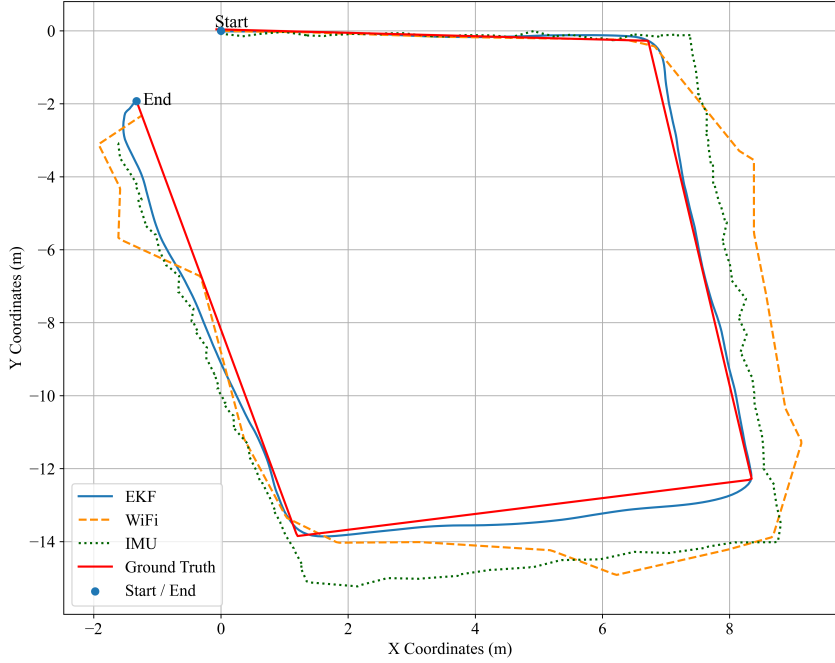


Figure 4.2: Comparison of experimental trajectories on the 7th floor

Table 4.1 shows the MSE and MAE calculated for this experiment relative to the EKF fusion method. For Wi-Fi localization, the experimental results show that the MAE of Wi-Fi is 1.1159 and the MSE is 1.9694, indicating that compared to EKF, Wi-Fi localization has a larger deviation and fluctuation in estimating spatial coordinates. The MAE of IMU localization is 0.9208, and the MSE is 1.8722, showing that IMU can provide relatively stable motion estimates in a short period of time. However, in long-term localization tasks, the error is still large, especially in rapidly changing environments.

Table 4.1: 7th floor localization accuracy evaluation

Localization Method	MAE (m)	MSE (m²)
Wi-Fi (w.r.t EKF)	1.1159	1.9694
IMU (w.r.t EKF)	0.9208	1.8722
EKF (w.r.t Ground Truth)	0.5690	0.9070

As shown in the Fig. 4.3, the maximum error of Wi-Fi localization and EKF fusion localization at a certain moment is displayed. Through the local magnification, we can see that the maximum Wi-Fi localization error mainly occurs in areas where signal attenuation and multipath effects are significant, which causes a large deviation in Wi-Fi localization.

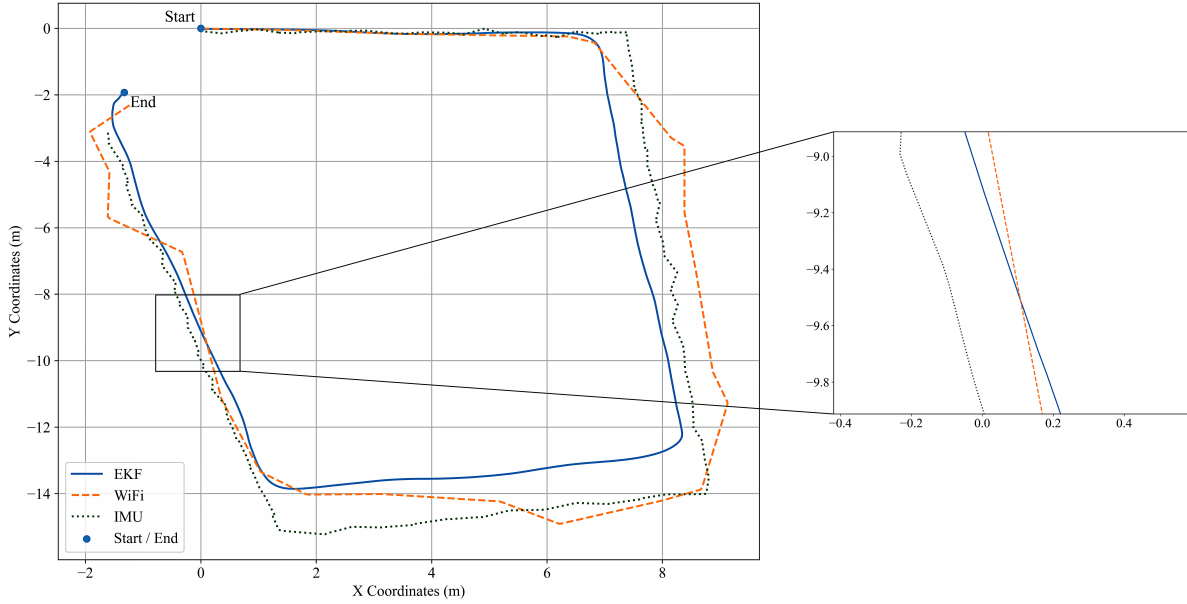


Figure 4.3: Amplified image of the error in the comparison of the experimental trajectories on the 7th floor

The following section presents the results of the experiment conducted on the 6th floor of the IR Building. Similar to the experiment on the 7th floor, this experiment compared the localization accuracy of different sensors and EKF under the same path conditions in this environment to evaluate the performance of different sensors and fusion methods in this environment.

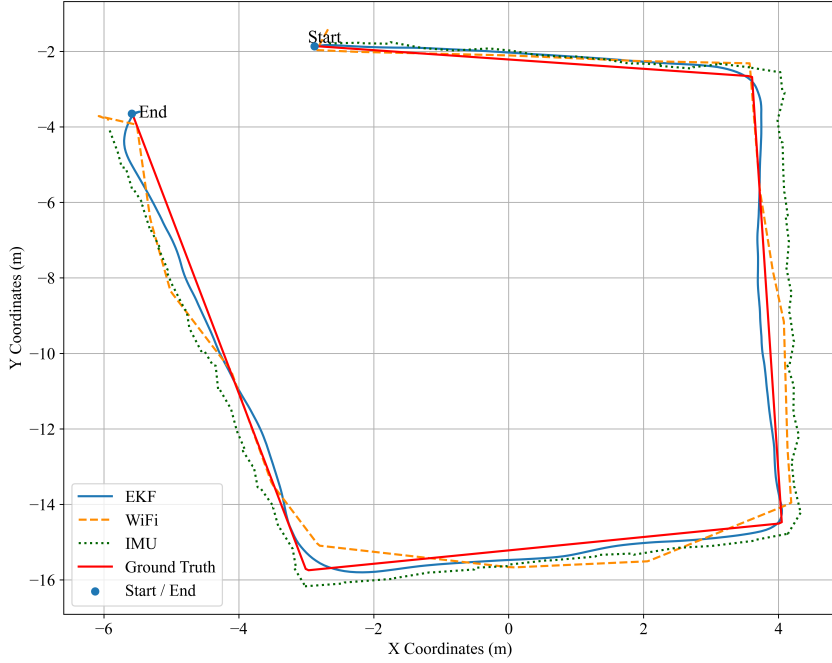


Figure 4.4: Comparison of experimental trajectories on the 6th floor

As can be seen from the Fig. 4.6, the trajectory results obtained on the 6th floor of the IR build-

ing are similar to the experimental results on the 7th floor. The drift of the Wi-Fi localization trajectory is relatively small, but due to signal frequency limitations, the trajectory still exhibits some smoothness issues. IMU localization showed a significant decrease in localization accuracy when turning corners. The EKF method effectively combines the advantages of Wi-Fi and IMU to provide a smoother and more accurate trajectory.

Table. 4.2 shows that in the experiment on the sixth floor, the accuracy of Wi-Fi localization was significantly improved compared with the test results on the seventh floor. Specifically, the MSE of Wi-Fi decreased from 1.9694 to 0.0855, and the MAE decreased from 1.1159 to 0.2335. In contrast, the localization accuracy of IMU did not change significantly, with MAE of 0.8801 and MSE of 1.7431.

Table 4.2: 6th floor localization accuracy evaluation (MAE and MSE)

Localization Method	MAE (m)	MSE (m^2)
Wi-Fi (w.r.t EKF)	0.2335	0.0855
IMU (w.r.t EKF)	0.8801	1.7431
EKF (w.r.t Ground Truth)	0.697	1.144

In addition, in order to analyze the specific situation of error distribution, the local enlarged view shown in Fig. 4.5 clearly shows the maximum error between Wi-Fi and EKF at certain moments. Through the local enlarged display, we can see that although the accuracy of Wi-Fi localization has been significantly improved, there are still errors between Wi-Fi and EKF. This further verifies that the EKF method can effectively fuse different sensor data in complex environments and provide more accurate and stable localization results.

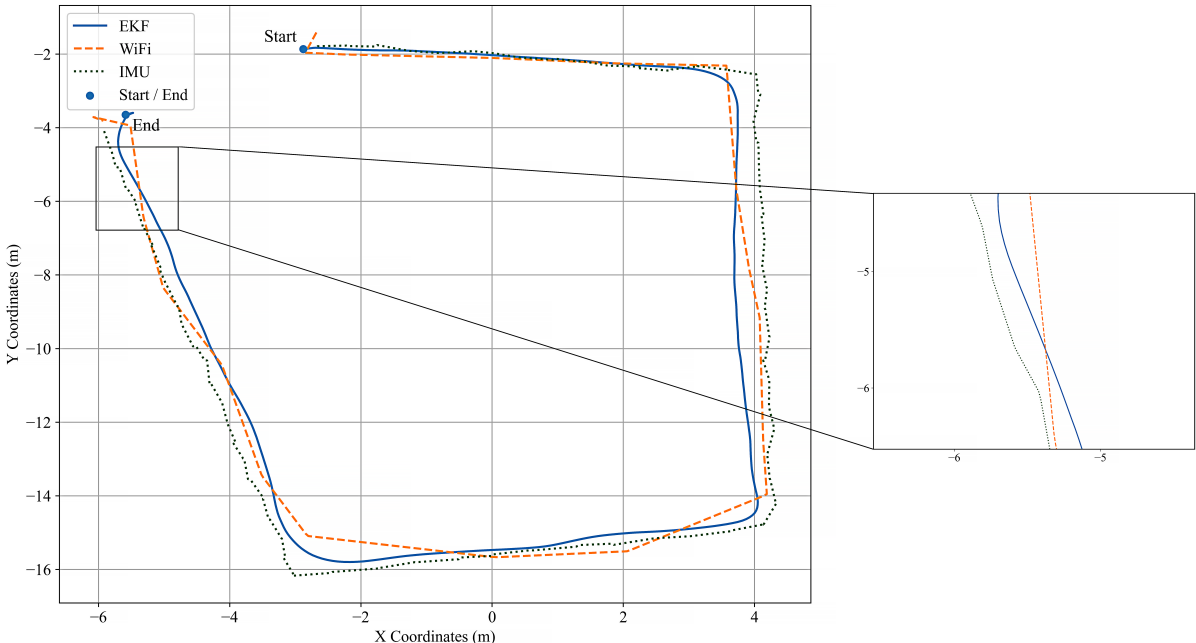


Figure 4.5: Amplified image of the error in the comparison of the experimental trajectories on the 6th floor

After completing the experimental analysis of the sixth and seventh floors, in order to further verify the generalization ability of the EKF fusion method, we conducted the same experiment on the eighth floor of the IR building.

As shown in the Fig. 4.6 of the experimental results on the 8th floor of the IR building, Wi-Fi localization is still affected by the signal environment, exhibiting a certain degree of drift, and the trajectory error is greater than that on the 6th floor. In addition, IMU localization is still inaccurate when turning corners and cannot stably capture the movement of the platform. In contrast, the EKF method effectively integrates Wi-Fi and IMU data, significantly improving localization performance and demonstrating greater robustness and stability in complex environments.

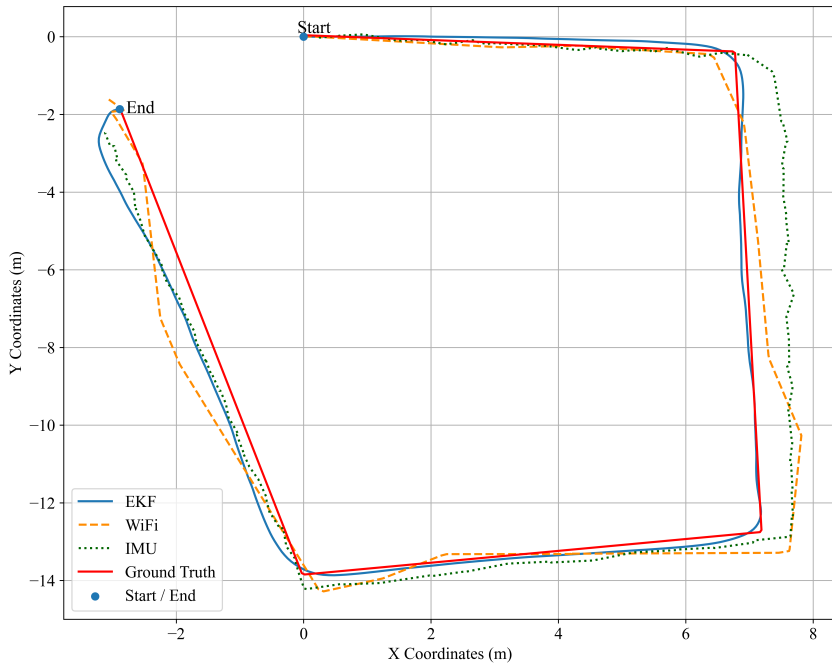


Figure 4.6: Comparison of experimental trajectories on the 8th floor

As shown in Table. 4.3, in the experiment on the 8th floor of the IR building, the MAE of Wi-Fi localization was 0.5846 and the MSE was 0.8358, indicating that the error of Wi-Fi localization varied greatly, with good and bad localization effects and considerable instability. This instability may be closely related to changes in the signal environment (such as signal obstruction and reflection), resulting in significant differences in the performance of Wi-Fi localization in different areas.

In contrast, the error variation range of the IMU is relatively small, with an MAE of 0.8645 and an MSE of 1.7970, indicating that the IMU maintains a relatively stable error level throughout the experiment. However, due to the inherent limitations of the sensors, the IMU's accuracy does not improve significantly in complex dynamic environments (such as when turning), resulting in larger errors, particularly during rapid movements.

Table 4.3: 8th floor localization accuracy evaluation (MAE and MSE)

Localization Method	MAE (m)	MSE (m^2)
Wi-Fi (w.r.t EKF)	0.5846	0.8358
IMU (w.r.t EKF)	0.8645	1.7970
EKF (w.r.t Ground Truth)	0.740	1.551

Based on the results of local magnification (Fig. 4.7), we conclude that the EKF method can effectively combine the advantages of Wi-Fi and IMU in similar environments on different floors. Through multiple corrections of sensor data, EKF significantly reduces the accumulation of errors and provides a smoother and more accurate localization trajectory.

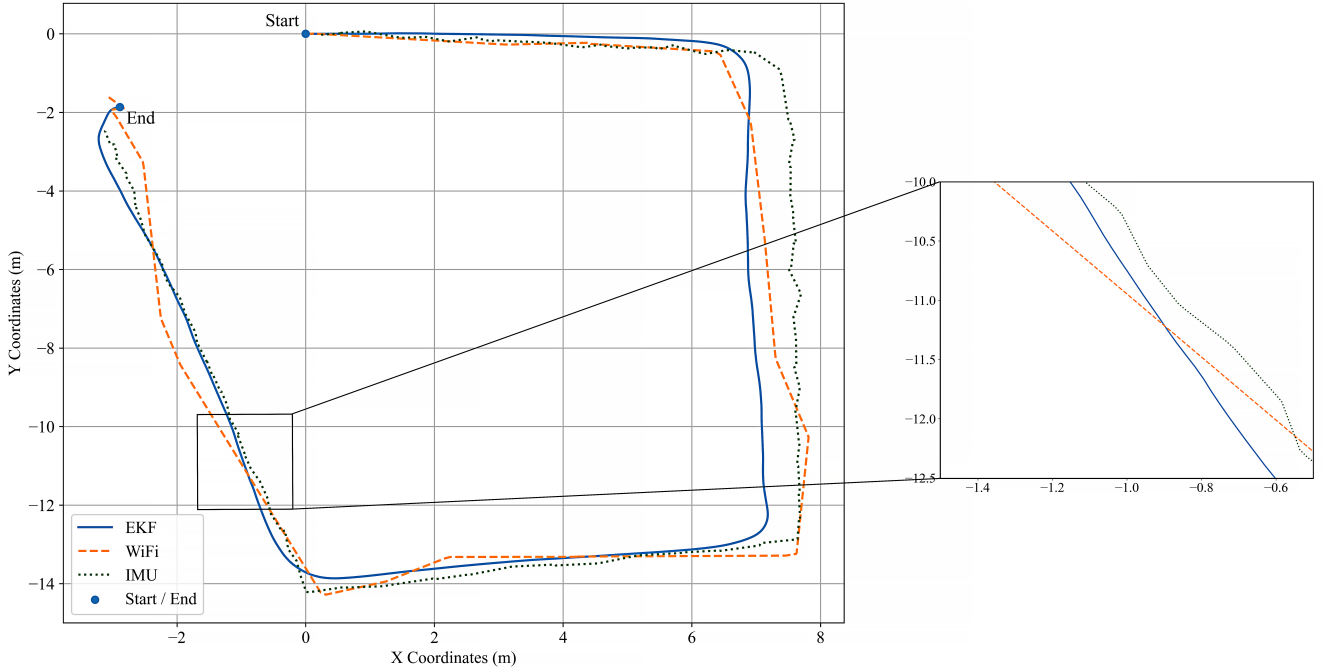


Figure 4.7: Amplified image of the error in the comparison of the experimental trajectories on the 8th floor

4.2 Full corridor trajectory evaluation on the 7th floor

In previous experiments, we conducted tests in similar corridor areas on the 6th, 7th, and 8th floors of the IR building. In order to further verify the stability and robustness of the system in different floor environments, this experiment was extended to the entire corridor area on the 7th floor. The specific trajectory is shown in Fig. 4.8. The purpose is to evaluate the localization accuracy and stability of the system over a larger area, especially in longer distances and more complex environments. By comparing the results with previous experiments conducted in similar areas, we can validate the system's adaptability across different spatial scales and

further evaluate the robustness and accuracy of different sensors and fusion methods in real-world applications.

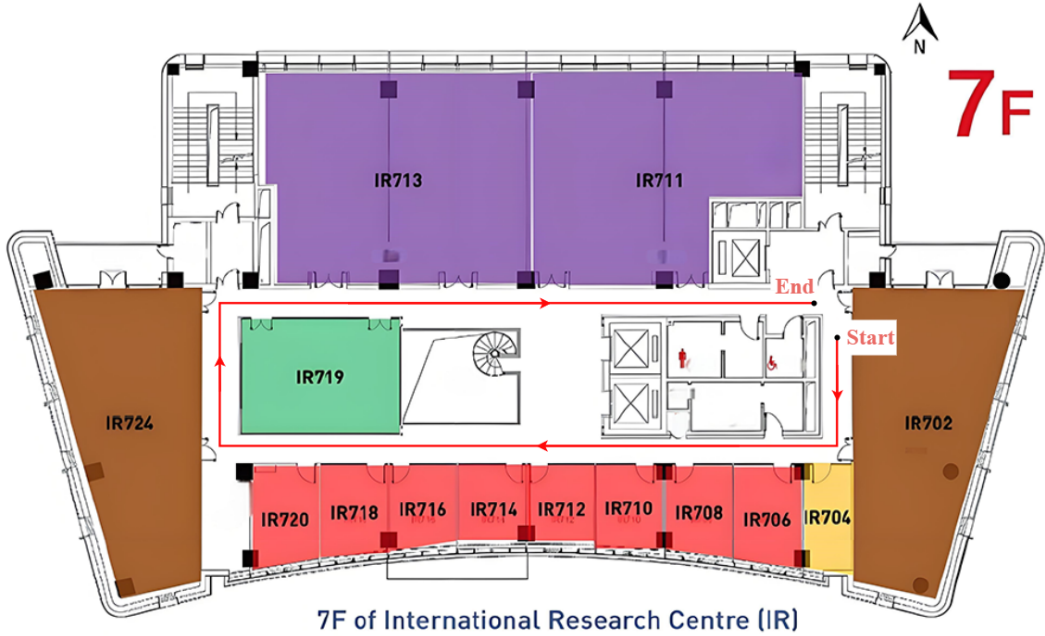


Figure 4.8: Second phase indoor localization experimental path

As can be seen from Fig. 4.9, Wi-Fi localization is greatly affected by the signal environment and exhibits obvious drift. Due to signal obstruction and the influence of smaller frequencies, the Wi-Fi localization trajectory is relatively tortuous and cannot provide a smooth trajectory. Especially on longer paths, the error is more significant, leading to a decrease in localization accuracy.

In contrast, IMU localization performs relatively smoothly throughout the entire path. Compared with Wi-Fi, IMU has less error accumulation and can maintain a relatively stable trajectory on longer paths. However, during rapid movement and turning, the localization accuracy of the IMU still decreases. Especially when the direction of movement changes significantly, IMU system errors begin to accumulate, leading to a further decrease in localization accuracy.

The EKF fusion method provides smoother and more accurate trajectories than single Wi-Fi and IMU localization methods. In areas with multiple turns and signal restrictions, EKF can effectively reduce errors and optimize localization results. By integrating information from different sensors, it compensates for their respective shortcomings and significantly improves localization accuracy.

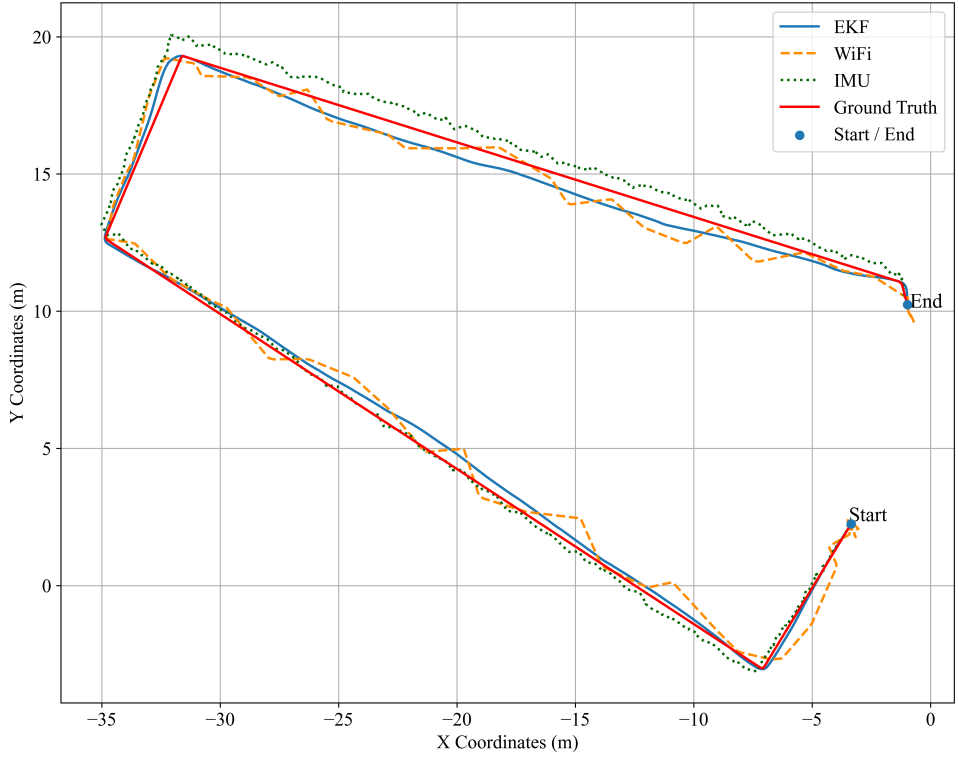


Figure 4.9: Comparison of experimental results trajectories in the entire corridor on the 7th floor of the IR building

According to Table. 4.1, the MAE of Wi-Fi localization is 0.2251 and the MSE is 0.0778, indicating that the overall error is small. However, Wi-Fi localization showed large fluctuations in the experiment, which was due to factors such as signal obstruction and reflection. Wi-Fi localization is based on RSSI signals, which are greatly affected by obstacles and multipath effects, resulting in uneven or tortuous trajectories in some areas. Nevertheless, Wi-Fi localization can still provide relatively accurate location estimates at some times, thereby maintaining low MAE and MSE values.

The MAE of the IMU is 0.6655, and the MSE is 0.8059, showing a reduction in error compared to previous experiments with shorter paths. This indicates that although errors still exist in longer paths, the overall error has improved compared to previous tests. The IMU can provide relatively stable platform position information, but error accumulation remains one of its main issues in dynamic environments. Through experiments on longer paths, the performance of the IMU in more complex environments can be verified, and it is further demonstrated that it can maintain relatively small errors under relatively stable conditions.

Table 4.4: Accuracy assessment of localization of entire path on 7th floor

Localization Method	MAE (m)	MSE (m^2)
Wi-Fi (w.r.t EKF)	0.2251	0.0778
IMU (w.r.t EKF)	0.6655	0.8059
EKF (w.r.t Ground Truth)	0.5290	0.6010

As shown in the enlarged view in Fig. 4.10, it can be clearly seen that the Wi-Fi localization trajectory has large fluctuations. At the same time, the IMU localization trajectory is slightly smoother than the Wi-Fi, but there are still errors. The IMU errors have a certain accumulation effect, causing the trajectory to deviate from the actual path. In comparison, it can be seen that the trajectory provided by EKF is smoother and more accurate than Wi-Fi and IMU.

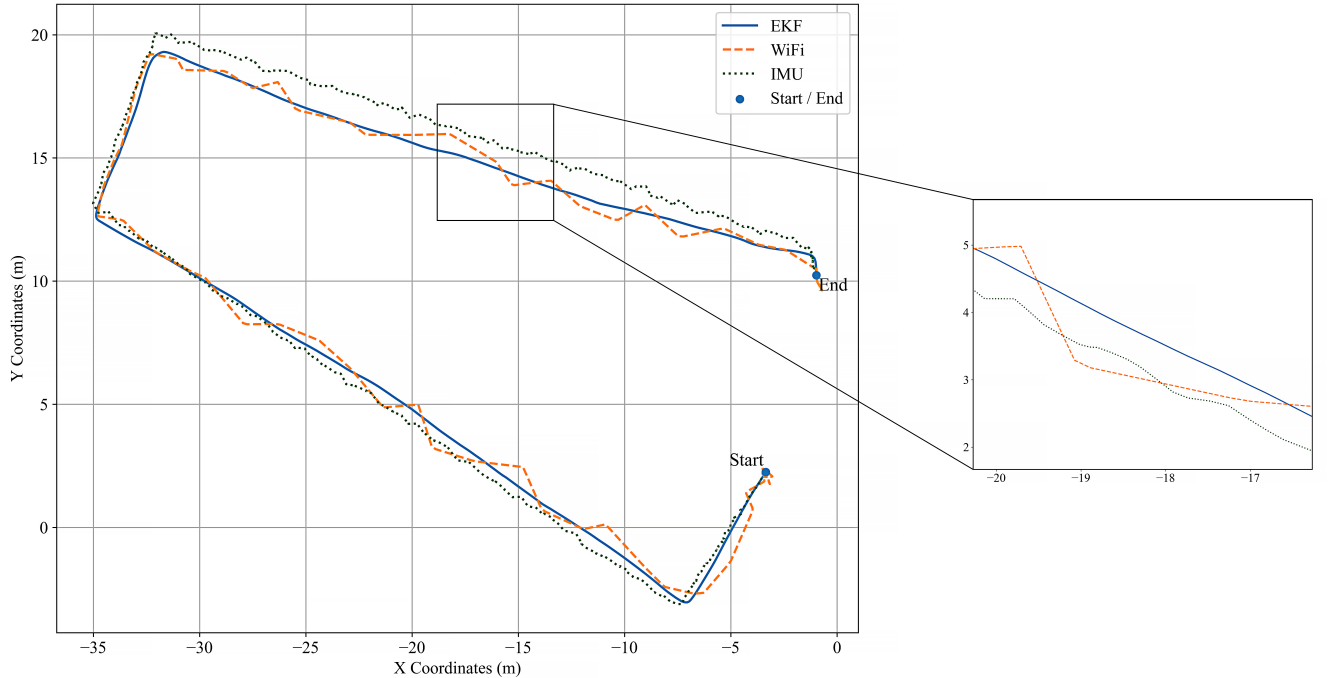


Figure 4.10: Enlarged image of the comparison error in the entire corridor on the 7th floor of the IR building

4.3 Evaluation under reversed start and end points

In the experiment above, we demonstrated the complete path experiment results on the 7th floor. In order to further verify the performance of the system at different start and end location, the path on the 7th floor was adjusted in this experiment, changing the start and end location, as shown in Fig. 4.11. Through this adjustment, we aimed to examine the localization consistency and accuracy of the system when the path direction changes, thereby further verifying its adaptability and robustness in practical applications.

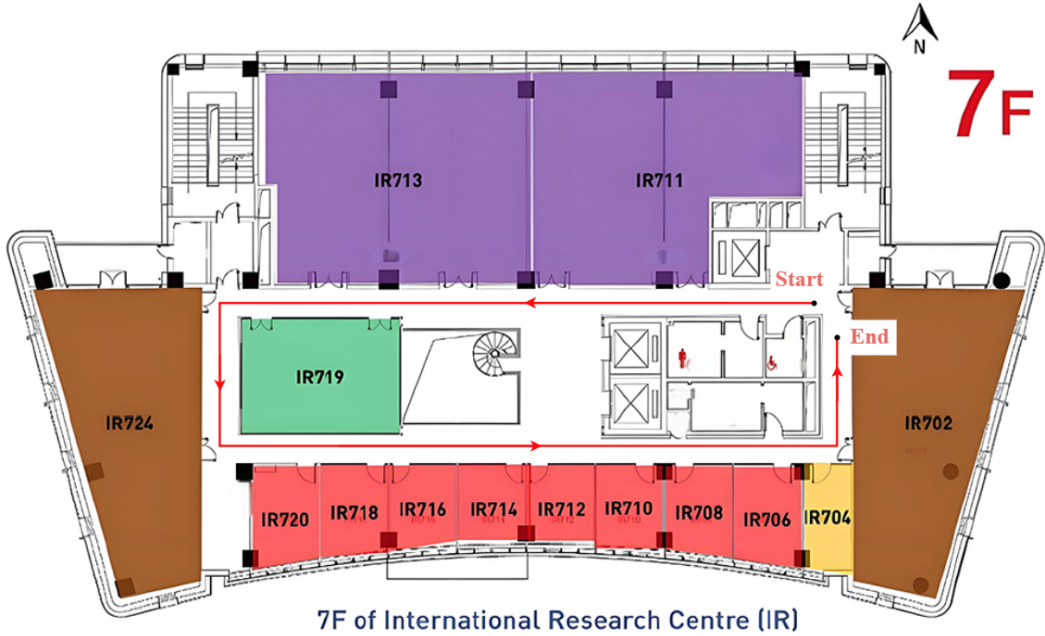


Figure 4.11: Indoor localization experiment path after changing location

Fig. 4.12 shows the comparison results of the trajectories obtained by swapping the starting and ending positions along the complete corridor path on the 7th floor of the IR building. The experimental path remains consistent with the previous complete corridor experiment, with only the direction of movement altered. This is aimed at evaluating the system's stability and consistency under changes in path direction.

As can be seen from Fig. 4.12, the Wi-Fi trajectory still exhibits significant fluctuations at the long path positions near the endpoint, indicating that it is susceptible to interference from signal obstruction or multipath effects and has poor stability. The IMU trajectory is generally smooth, but error accumulation still occurs during long path travel, causing the trajectory to deviate from the actual path gradually. In contrast, the EKF fusion method maintains stable, continuous, and accurate path estimation even after changing the path direction, fully demonstrating its robustness and adaptability to changes in travel direction and environmental conditions under multi-source information fusion.

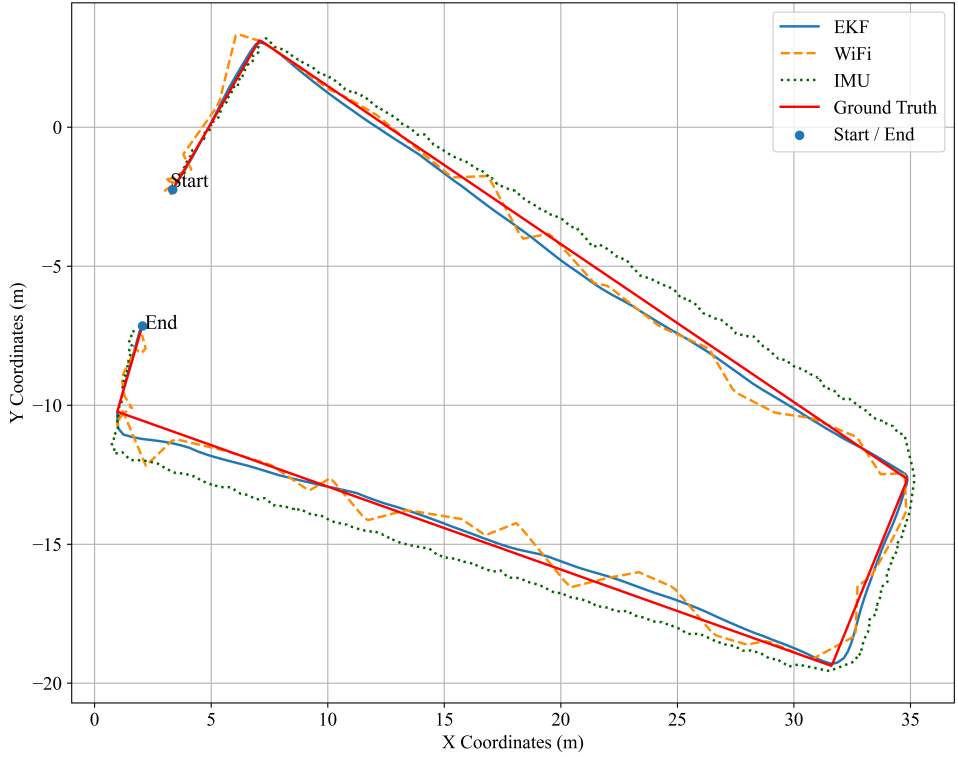


Figure 4.12: Complete path comparison of IR building 7th floor experiment trajectory (start and end locations swapped)

In the experiment where the starting and ending positions of the complete corridor path were swapped, the error metrics of Wi-Fi and IMU exhibited trends consistent with previous experiments but also showed some differences. As shown in Table 4.5, the Wi-Fi MAE was 0.2493 and the MSE was 0.1038, slightly higher than the MAE (0.2251) and MSE (0.0778) obtained in the previous experiment with the same path but in the opposite direction. This indicates that Wi-Fi became slightly more sensitive to changes in the local signal environment after the path direction was changed, with more significant fluctuations observed near the start and end regions.

The MAE and MSE of IMU are 0.8494 and 1.1384, respectively. Although they still exhibit a trend of error accumulation over time, they have increased compared to the previous experiment's MAE (0.6655) and MSE (0.8059), indicating that the change in travel direction may have exacerbated the cumulative effect of attitude estimation errors at different turning nodes. Overall, although Wi-Fi and IMU exhibited some degree of error fluctuation under changes in the direction of travel, the EKF fusion method maintained good stability and accuracy in this experiment.

Table 4.5: 7th floor inverse-path localization accuracy evaluation (MAE and MSE)

Localization Method	MAE (m)	MSE (m^2)
Wi-Fi (w.r.t EKF)	0.2493	0.1038
IMU (w.r.t EKF)	0.8494	1.1384
EKF (w.r.t Ground Truth)	0.8830	1.9050

Fig. 4.13 shows a magnified view of the complete path experiment after swapping the start and end positions, focusing on the corner area where Wi-Fi errors are relatively large. As can be seen from the figure, the Wi-Fi trajectory shows a significant deviation in this section, with a huge trajectory jump at the corner. The IMU trajectory, on the other hand, exhibits a relatively smooth trend overall, but also shows signs of error accumulation in this area, primarily manifested as a continuous deviation in the trajectory. In contrast, the EKF fusion trajectory maintains good smoothness and spatial consistency in this area, accurately following the actual movement path.

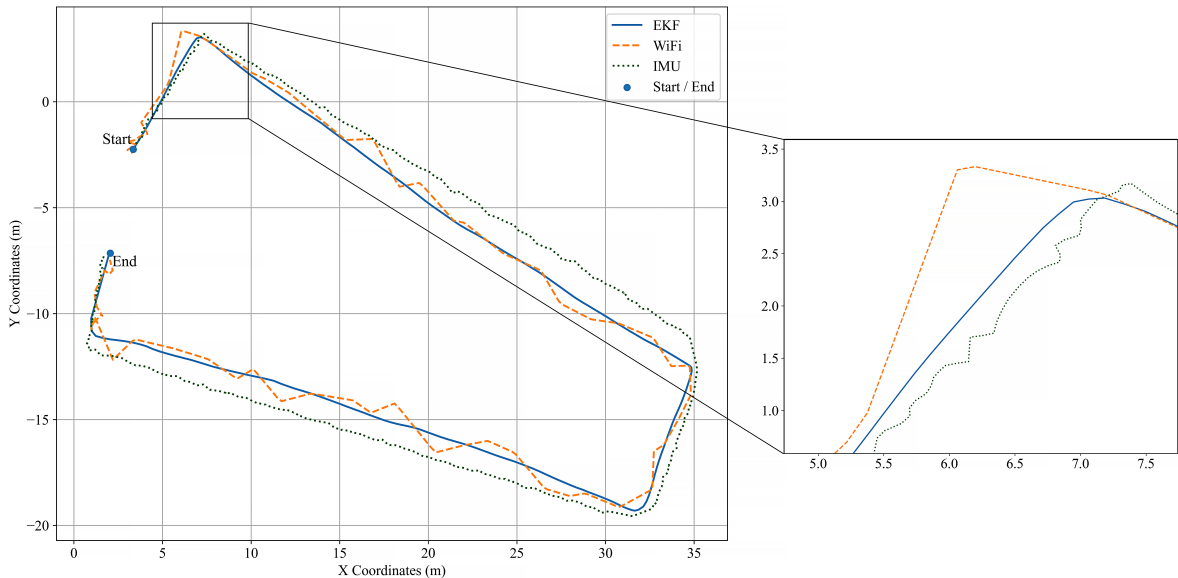


Figure 4.13: Enlarged image of the comparison error in the entire corridor on the 7th floor of the IR building (start and end locations swapped)

5 Discussion and Limitations

Despite the demonstrated effectiveness of the proposed fusion localization framework, several limitations remain that warrant further investigation:

- **Instability and limited generalization of Wi-Fi fingerprinting:** Although the Wi-Fi fingerprinting model performs robustly in most areas, the RSSI is highly susceptible to multipath propagation, obstruction, and environmental variations. These factors introduce considerable measurement uncertainty and hinder the model's generalization across

different locations. In particular, localization accuracy degrades significantly in areas with sparse reference points or strong signal occlusion. Additionally, the low update rate of Wi-Fi signals—typically on the order of seconds—limits the system’s responsiveness to rapid platform dynamics, resulting in delayed positional updates during fast movement or turning.

- **Drift and error accumulation in IMU measurements:** The inertial measurement unit (IMU) provides high-frequency motion data with strong short-term responsiveness. However, its accelerometers and gyroscopes are vulnerable to noise and bias drift, leading to cumulative errors over time. Without timely correction from external observations (e.g., SLAM), the IMU’s estimations diverge from the true trajectory, which negatively affects the overall accuracy and robustness of the system.
- **Sensitivity of SLAM to dynamic and occluded environments:** Although SLAM contributes mid-frequency structural constraints, its loop-closure performance can be compromised in dynamic scenes or environments with significant occlusions. This weakens the consistency and accuracy of the state updates performed by the EKF.
- **Limited diversity in experimental settings:** The experiments were conducted in campus buildings characterized by long corridors and regular spatial layouts. While representative, the system’s adaptability to open spaces, highly dynamic settings, or crowded public environments remains unverified. Further studies should extend the evaluation to more diverse and challenging scenarios.
- **Lack of adaptive parameter tuning in the EKF model:** The performance of the system relies heavily on the manual configuration of EKF parameters, particularly the process and measurement noise covariance matrices. These parameters significantly influence the filter’s convergence and localization accuracy. Future work should consider the integration of adaptive tuning strategies, such as Bayesian optimization or reinforcement learning, to enhance the model’s adaptability and reduce dependency on manual calibration.

6 Conclusion and Future work

6.1 Conclusion

In summary, this study proposes and evaluates a robust multi-sensor indoor localization system. The main conclusions are as follows:

- **A novel fusion framework** was developed by integrating Wi-Fi fingerprinting, Lidar-based SLAM, and EKF, effectively addressing the limitations of single-modality localization in complex indoor environments.

- **The DNN-based Wi-Fi localization approach** successfully captures the nonlinear relationship between RSSI and spatial position, resulting in improved localization accuracy over traditional methods.
- **The Gmapping-based SLAM algorithm** enables efficient real-time environment mapping and localization, enhancing the system's adaptability and robustness in dynamic and cluttered environments.
- **The EKF-based data fusion module** significantly improves localization stability by suppressing Wi-Fi signal fluctuations and mitigating IMU drift, leading to more accurate and smooth trajectory estimation.
- **Extensive real-world experiments** were conducted across multiple floors and diverse routes, validating the system's performance, generalizability, and feasibility for practical deployment in real indoor environments.

6.2 Future Work

Given the limitations of this study, future work can be further expanded and optimized in the following directions:

- **Enhancing system robustness:** More heterogeneous sensors, such as UWB, visual information, or BLE, can be introduced to enhance the system's adaptability to complex indoor environments, multi-path interference, and signal occlusion, thereby improving its robustness in response to environmental fluctuations.
- **3d Lidar and advanced SLAM integration:** Future research may consider upgrading the 2D Lidar to a 3d Lidar sensor and combining it with real-time point cloud processing technologies. More advanced SLAM algorithms, such as FAST-LIO2, can be introduced to construct high-precision, high-robustness 3d maps, improving the system's perception and localization capabilities in multi-floor and multi-structure environments.
- **Incorporating deep learning models:** Deep learning techniques, particularly temporal modelling structures such as RNNs, GRUs, or Transformers, can be applied to estimate localization trajectories in an end-to-end manner. This would enhance the system's ability to model non-linear and dynamic state transitions. Additionally, exploring self-supervised or weakly supervised learning frameworks could reduce reliance on labelled trajectory datasets.
- **Online learning and incremental mapping:** Incorporating online learning mechanisms and incremental map updating strategies could further improve the system's adaptability during long-term deployment, enabling continuous optimization of localization accuracy and environmental modelling.

- **Embedded deployment and system validation:** The current system could be ported to an embedded platform (e.g., NVIDIA Jetson Orin Nano) to perform real-time testing. This would allow for a comprehensive evaluation of the system’s power consumption, resource scheduling efficiency, and latency performance, laying a foundation for practical deployment in mobile robotics and indoor navigation applications.

References

- [1] L. Yang, N. Wu, B. Li, W. Yuan, and L. Hanzo, “Indoor localization based on factor graphs: A unified framework,” *IEEE Internet of Things Journal*, vol. PP, pp. 1–1, 01 2022.
- [2] N. H. A. Wahab, N. Sunar, S. H. Ariffin, K. Y. Wong, Y. Aun *et al.*, “Indoor positioning system: A review,” *International Journal of Advanced Computer Science and Applications*, vol. 13, no. 6, 2022.
- [3] X. Guo, N. Ansari, F. Hu, Y. Shao, N. R. Elikplim, and L. Li, “A survey on fusion-based indoor positioning,” *IEEE Communications Surveys & Tutorials*, vol. 22, no. 1, pp. 566–594, 2019.
- [4] A. M. Hossain and W.-S. Soh, “A survey of calibration-free indoor positioning systems,” *Computer Communications*, vol. 66, pp. 1–13, 2015.
- [5] C. Fischer and H. Gellersen, “Location and navigation support for emergency responders: A survey,” *IEEE Pervasive Computing*, vol. 9, no. 01, pp. 38–47, 2010.
- [6] Y. Zhang and Z. Chen, “Smart cities: A survey on indoor localization technologies and applications,” *IEEE Access*, vol. 8, pp. 30 398–30 410, 2020.
- [7] H. Chen, J. Wang, and Y. Li, “Indoor localization in retail industry: Applications and challenges,” *IEEE Transactions on Industrial Informatics*, vol. 15, no. 6, pp. 3457–3468, 2019.
- [8] R. J. Fontana, “Recent system applications of short-pulse ultra-wideband (uwb) technology,” *IEEE Transactions on microwave theory and techniques*, vol. 52, no. 9, pp. 2087–2104, 2004.
- [9] P. S. Farahsari, A. Farahzadi, J. Rezazadeh, and A. Bagheri, “A survey on indoor positioning systems for iot-based applications,” *IEEE Internet of Things Journal*, vol. 9, no. 10, pp. 7680–7699, 2022.
- [10] S. Yiu, M. Dashti, H. Claussen, and F. Perez-Cruz, “Wireless rssi fingerprinting localization,” *Signal Processing*, vol. 131, pp. 235–244, 2017.

- [11] F. Gustafsson and F. Gunnarsson, “Positioning using time-difference of arrival measurements,” in *2003 IEEE International Conference on Acoustics, Speech, and Signal Processing, 2003. Proceedings.(ICASSP’03)., vol. 6.* IEEE, 2003, pp. VI–553.
- [12] H. Yan, Q. Shan, and Y. Furukawa, “Ridi: Robust imu double integration,” in *Proceedings of the European conference on computer vision (ECCV)*, 2018, pp. 621–636.
- [13] R. Jirawimut, P. Ptasinski, V. Garaj, F. Cecelja, and W. Balachandran, “A method for dead reckoning parameter correction in pedestrian navigation system,” *IEEE Transactions on Instrumentation and Measurement*, vol. 52, no. 1, pp. 209–215, 2003.
- [14] F. Caron, E. Duflos, D. Pomorski, and P. Vanheeghe, “Gps/imu data fusion using multisensor kalman filtering: introduction of contextual aspects,” *Information fusion*, vol. 7, no. 2, pp. 221–230, 2006.
- [15] O. Dehzangi, M. Taherisadr, and R. ChangalVala, “Imu-based gait recognition using convolutional neural networks and multi-sensor fusion,” *Sensors*, vol. 17, no. 12, p. 2735, 2017.
- [16] J. Marins *et al.*, “Improved inertial navigation with multi-sensor fusion,” *IEEE Transactions on Robotics*, vol. 17, no. 6, pp. 1338–1344, 2001.
- [17] Y. Wu *et al.*, “Indoor localization system based on imu and wifi,” *Sensors*, vol. 15, no. 7, pp. 17 947–17 960, 2015.
- [18] X. Liu, B. Zhou, P. Huang, W. Xue, Q. Li, J. Zhu, and L. Qiu, “Kalman filter-based data fusion of wi-fi rtt and pdr for indoor localization,” *IEEE Sensors Journal*, vol. 21, no. 6, pp. 8479–8490, 2021.
- [19] F. Liu, J. Liu, Y. Yin, W. Wang, D. Hu, P. Chen, and Q. Niu, “Survey on WiFi-based indoor positioning techniques,” *IET communications*, vol. 14, no. 9, pp. 1372–1383, 2020.
- [20] Y. Jiang *et al.*, “Indoor localization system based on wi-fi fingerprint and environmental adaptability,” *Sensors*, vol. 19, no. 7, pp. 1556–1578, 2019.
- [21] L. Li *et al.*, “Calibration-free indoor localization: A review,” *IEEE Access*, vol. 6, pp. 64 129–64 142, 2018.
- [22] T. Zhang *et al.*, “Robust indoor localization based on wi-fi fingerprinting and optimization techniques,” *IEEE Transactions on Mobile Computing*, vol. 19, no. 7, pp. 1789–1800, 2020.
- [23] C. Laoudias, A. Moreira, S. Kim, S. Lee, L. Wirola, and C. Fischione, “A survey of enabling technologies for network localization, tracking, and navigation,” *IEEE Communications Surveys & Tutorials*, vol. 20, no. 4, pp. 3607–3644, 2018.

- [24] X. Xu *et al.*, “Wireless localization in complex environments: A survey,” *IEEE Communications Surveys & Tutorials*, vol. 21, no. 2, pp. 1295–1320, 2019.
- [25] G. M. Mendoza-Silva, P. Richter, J. Torres-Sospedra, E. S. Lohan, and J. Huerta, “Long-term wifi fingerprinting dataset for research on robust indoor positioning,” *Data*, vol. 3, no. 1, 2018.
- [26] H. Zhang *et al.*, “Dynamic fingerprint update for indoor localization,” *IEEE Sensors Journal*, vol. 19, no. 6, pp. 2202–2214, 2019.
- [27] A. Filieri, H. Hoffmann, and M. Maggio, “Automated design of self-adaptive software with control-theoretical formal guarantees,” in *Proceedings of the 36th International Conference on Software Engineering*, ser. ICSE 2014. New York, NY, USA: Association for Computing Machinery, 2014, p. 299–310.
- [28] S. Sen, J. Lee, K.-H. Kim, and P. Congdon, “Avoiding multipath to revive inbuilding wifi localization,” in *MobiSys*, 2013, pp. 249–262.
- [29] Y. Shang, J. Weng, and J. Wang, “Enhancing indoor localization using social wi-fi data,” *IEEE Transactions on Mobile Computing*, vol. 14, no. 7, pp. 1309–1322, 2015.
- [30] X. He, D. N. Aloisio, and J. Li, “Probabilistic multi-sensor fusion based indoor positioning system on a mobile device,” *Sensors*, vol. 15, no. 12, pp. 31 464–31 481, 2015.
- [31] M. Nowicki and J. Wietrzykowski, “Low-effort place recognition with wifi fingerprints using deep learning,” in *International Conference on Automation, Control and Robotics (ICACR)*, 2017, pp. 1–6.
- [32] S. Xia, Y. Liu, G. Yuan, M. Zhu, and Z. Wang, “Indoor fingerprint positioning based on Wi-Fi: An overview,” *ISPRS International Journal of Geo-Information*, vol. 6, no. 5, 2017.
- [33] H. Zou *et al.*, “Magloc: Magnetometer-based indoor localization using deep neural networks,” *IEEE Transactions on Mobile Computing*, vol. 21, no. 1, pp. 145–159, 2022.
- [34] H. Zhou *et al.*, “A deep learning framework for robust indoor localization using lstm and multi-sensor fusion,” *Sensors*, vol. 22, no. 4, p. 1654, 2022.
- [35] A. Barrau, “Non-linear state error based extended kalman filters with applications to navigation,” Ph.D. dissertation, Mines Paristech, 2015.
- [36] P. Zhou, H. Wang, R. Gravina, and F. Sun, “Wio-ekf: Extended kalman filtering-based wi-fi and inertial odometry fusion method for indoor localization,” *IEEE Internet of Things Journal*, vol. 11, no. 13, pp. 23 592–23 603, 2024.

- [37] F. Zafari, A. Gkelias, and K. K. Leung, “A survey of indoor localization systems and technologies,” *IEEE Communications Surveys & Tutorials*, vol. 21, no. 3, pp. 2568–2599, 2019.
- [38] K. Liu and et al., “Fusion of wi-fi, inertial and magnetic sensors for indoor localization using deep learning,” *IEEE Sensors Journal*, vol. 19, no. 13, pp. 4821–4830, 2019.
- [39] Y. Gu and et al., “Uwb and lidar data fusion for indoor mobile robot localization,” *Sensors*, vol. 20, no. 8, p. 2345, 2020.
- [40] H. Durrant-Whyte and T. Bailey, “Simultaneous localization and mapping: part i,” *IEEE robotics & automation magazine*, vol. 13, no. 2, pp. 99–110, 2006.
- [41] G. Grisetti, C. Stachniss, and W. Burgard, “Improved techniques for grid mapping with rao-blackwellized particle filters,” in *IEEE Transactions on Robotics*, vol. 23, no. 1, 2007, pp. 34–46.
- [42] Y. Zhuang, X. Sun, Y. Li, J. Huai, L. Hua, X. Yang, X. Cao, P. Zhang, Y. Cao, L. Qi *et al.*, “Multi-sensor integrated navigation/positioning systems using data fusion: From analytics-based to learning-based approaches,” *Information Fusion*, vol. 95, pp. 62–90, 2023.
- [43] T. Bailey, J. Nieto, J. Guivant, M. Stevens, and E. Nebot, “Consistency of the ekf-slam algorithm,” in *2006 IEEE/RSJ International Conference on Intelligent Robots and Systems*. IEEE, 2006, pp. 3562–3568.
- [44] D. Lerro and Y. Bar-Shalom, “Tracking with debiased consistent converted measurements versus ekf,” *IEEE transactions on aerospace and electronic systems*, vol. 29, no. 3, pp. 1015–1022, 1993.
- [45] M. Li and A. I. Mourikis, “High-precision, consistent ekf-based visual-inertial odometry,” *The International Journal of Robotics Research*, vol. 32, no. 6, pp. 690–711, 2013.
- [46] B. Li, J. Salter, A. Dempster, and C. Rizos, “Indoor positioning techniques based on wireless lan,” in *IEEE International Conference on Wireless Broadband and Ultra Wideband Communications*, 2006.
- [47] Y. Sun, X. Li, H. Zhang, and M. Wang, “Fusion positioning algorithm using wifi and imu based on ekf,” *IEEE Access*, vol. 7, pp. 34 475–34 485, 2019.
- [48] S. He and S. Chan, “Wi-fi fingerprint-based indoor positioning: Recent advances and comparisons,” *IEEE Communications Surveys & Tutorials*, vol. 18, no. 1, pp. 466–490, 2016.